DocuServe

Electronic Delivery Cover Sheet

Caltech Library Services

ELSEVIER

Computer Physics Communications 113 (1998) 49–77

Computer Physics Communications

Heterostructures of photonic crystals: frequency bands and transmission coefficients

N. Stefanou [a,1], V. Yannopapas [a,2], A. Modinos [b]

[a] *University of Athens, Section of Solid State Physics, Panepistimioupolis, GR-157 84 Athens, Greece*

[b] *Department of Physics, National Technical University of Athens, Zografou Campus, GR-157 73 Athens, Greece*

Received 16 April 1998

Abstract

We present a program for the calculation of the frequency band structure of an infinite photonic crystal, and of the transmission, reflection and absorption coefficients of light by a slab of this crystal. The crystal consists of a stack of identical slices parallel to a given surface; a slice may consist of a number of different components, each of which can be either a homogeneous plate or a multilayer of spherical particles of given periodicity parallel to the surface. © 1998 Elsevier Science B.V.

PACS: 42.70.Qs; 42.25.Bs; 68.65.+g

Keywords: Photonic crystals; Complex photonic band structure; Transmission and reflection coefficients; Multiple scattering of electromagnetic waves

PROGRAM SUMMARY

Title of program: MULTEM

Catalogue identifier: ADIM

Program Summary URL:
http://www.cpc.cs.qub.ac.uk/cpc/summaries/ADIM

Program obtainable from: CPC Program Library, Queen's University of Belfast, N. Ireland

Licensing provisions: none

Computer for which the program is designed and others on which it is operable: *Computers:* HP Apollo 9000/720,715,735, Pentium PC; *Installation:* University of Athens, Section of Solid State Physics

Operating systems under which the program has been tested: HP-UX, LINUX

Programming language used: FORTRAN 77

Memory required to execute with typical data: 1.15 Mbytes

No. of bits in a word: 32

No. of bytes in distributed program, including test data, etc.: 149265

Distribution format: ASCII

[1] E-mail: nstefan@atlas.uoa.gr.

[2] Supported by the State Scolarships Foundation (I.K.Y.), Greece.

PII S0010-4655(98)00060-5

Keywords: Photonic crystals, complex photonic band structure, transmission and reflection coefficients, multiple scattering of electromagnetic waves

Nature of physical problem
Calculation of the complex band structure associated with a given surface of a photonic crystal, and of the transmission, reflection and absorption coefficients of light by a slab of the crystal parallel to the given surface. We note that the ordinary frequency band structure of the infinite crystal is contained within the complex band structure of any surface of the crystal.

Method of solution
Solution of Maxwell's equations using multiple-scattering techniques.

Restrictions on the complexity of the problem
The structures that can be considered consist of parallel planes of non-overlapping spheres of given two-dimensional periodicity and uniform plates.

Typical running time
For the given test run, about 26 s per frequency for the band structure calculation and 54 s per frequency for the transmission/reflection/absorption calculation, on an HP Apollo 9000/735.

LONG WRITE-UP

1. Introduction

Photonic crystals are composite materials with a dielectric function $\epsilon(\boldsymbol{r},\omega)\epsilon_0$ which is a periodic function of the position $\boldsymbol{r}$, with a period comparable to the wavelength of light [1]. A most interesting aspect of such materials arises from the possibility of frequency regions, known as (absolute) photonic gaps, over which there can be no propagation of light in the crystal whatever the direction of propagation; a phenomenon which can have many and important applications in optoelectronics [2]. So far it has been possible to fabricate photonic crystals with absolute frequency gaps in the region up to 4 THz [3] and further progress to higher frequencies is expected. And there may be applications of photonic crystals which do not relate directly to the existence of photonic gaps [4]. For a recent review of photonic crystals and their applications the reader is referred to [5].

Among the methods suggested for the calculation of frequency bands, the so-called on-shell methods appear to be numerically efficient and at the same time allow the calculation of the transmission/reflection coefficient of light (of given frequency) incident on a slab of the photonic crystal [6–11]. The computer program which we present here is based on our method of calculating frequency bands and transmission coefficients [9]. The method allows us to treat slabs which consist of slices of different material as long as the periodicity parallel to the surface of the slab is preserved (see below). The basic components of a slice can be either homogeneous plates or multilayers of non-overlapping spheres. Although the spherical shape of the scatterers constitutes a limitation of our method, it still allows for a great variety of structures, and we hope that it will be a useful tool in further exploration of the possibilities of heterostructures of photonic crystals.

In our method, like in other on-shell methods, the dielectric function of the scatterer is in general a function (possibly complex) of the frequency. In cases where the dielectric function has an imaginary part, all waves in the crystal are of course evanescent waves. Our method calculates these waves and also the experimentally measured quantities: the reflection, transmission, and the absorption of the incident radiation by a slab of the material. The structures that can be dealt with by our program are described below. They have a two-dimensional (2D) periodicity in the xy-plane and, therefore, the xy-component of the wavevector, $\boldsymbol{k}_{\|}$, modulo a 2D reciprocal-lattice vector is an invariant.

One can have a finite (in the z-direction) slab consisting of a number of *unit slices* (unit supercells), embedded in a homogeneous medium characterized by a real dielectric function and a real magnetic permeability. In this case, the program calculates the transmission, reflection and absorption coefficients for a plane electromagnetic (EM) wave, incident on the slab from the left. The Fourier components of the transmitted and reflected fields are also available.

Alternatively, one can calculate the complex photonic band structure of an infinite crystal, generated by a primitive translation of the unit slice. In this case the program provides the propagating and evanescent eigenmodes of the EM field in the given crystal, corresponding to a given $\boldsymbol{k}_{\parallel}$ and a given frequency.

The unit slice consists of a number of different *components*, each of which can be either a *homogeneous plate*, or a *multilayer of spherical particles* in a homogeneous host medium. The multilayer is a stack of identical layers, each of which consists, in general, of a number of different (non-primitive) *planes of spheres* with the same 2D periodicity. We note that the separation of two successive planes of a multilayer (given by the z-component of the vector which joins the centres of the two planes) needs only be larger than the radii of the spheres of the two planes, as long as there is no overlap between the spheres. If the host media of two successive components (belonging to the same or successive slices) are not the same, their interface is taken into account by introducing it as an additional component. We note, however, that the (planar) interface must not cut any spheres. A structure typical of the ones that can be treated by our program is presented in Section 4.

2. Theory

2.1. Scattering of a plane wave by a sphere

A plane EM wave of angular frequency ω and wavevector $\boldsymbol{q}$, propagating in a homogeneous medium characterized by a real dielectric function $\epsilon(\omega)\epsilon_0$ and a real magnetic permeability $\mu(\omega)\mu_0$, where ϵ_0, μ_0 are the dielectric constant and the magnetic permeability of vacuum, has an electric-field component

$$\boldsymbol{E}(\boldsymbol{r},t) = \mathrm{Re}\left[\boldsymbol{E}(\boldsymbol{r})\exp(-\mathrm{i}\omega t)\right] \tag{1}$$

and a magnetic-field component

$$\boldsymbol{H}(\boldsymbol{r},t) = \mathrm{Re}\left[\boldsymbol{H}(\boldsymbol{r})\exp(-\mathrm{i}\omega t)\right], \tag{2}$$

defined by

$$\boldsymbol{E}(\boldsymbol{r}) = \boldsymbol{E}_0(\boldsymbol{q})\exp(\mathrm{i}\boldsymbol{q}\cdot\boldsymbol{r}) \tag{3}$$

and

$$\boldsymbol{H}(\boldsymbol{r}) = -\left(\frac{\mathrm{i}}{\omega\mu\mu_0}\right)\nabla\times\boldsymbol{E}(\boldsymbol{r}). \tag{4}$$

The magnitude of the wavevector is given by $q = \sqrt{\mu\epsilon}\,\omega/c$, where $c = 1/\sqrt{\mu_0\epsilon_0}$ is the velocity of light in vacuum. $\boldsymbol{E}_0(\boldsymbol{q}) \equiv E_0(\boldsymbol{q})\hat{\boldsymbol{p}}$, where E_0 denotes the magnitude and $\hat{\boldsymbol{p}}$, a unit vector, the polarization of the electric field. The above plane wave can be expanded in spherical waves as follows [7]:

$$\boldsymbol{E}(\boldsymbol{r}) = \sum_{\ell=1}^{\infty}\sum_{m=-\ell}^{\ell}\left(\frac{\mathrm{i}}{q}\mathrm{a}_{\ell m}^{0E}\nabla\times j_\ell(qr)\boldsymbol{X}_{\ell m}(\hat{\boldsymbol{r}}) + \mathrm{a}_{\ell m}^{0H} j_\ell(qr)\boldsymbol{X}_{\ell m}(\hat{\boldsymbol{r}})\right). \tag{5}$$

The corresponding formula for the associated magnetic field is obtained by substituting Eq. (5) into Eq. (4),

$$\boldsymbol{H}(\boldsymbol{r}) = \sqrt{\frac{\epsilon\epsilon_0}{\mu\mu_0}}\sum_{\ell=1}^{\infty}\sum_{m=-\ell}^{\ell}\left(\mathrm{a}_{\ell m}^{0E} j_\ell(qr)\boldsymbol{X}_{\ell m}(\hat{\boldsymbol{r}}) - \frac{\mathrm{i}}{q}\mathrm{a}_{\ell m}^{0H}\nabla\times j_\ell(qr)\boldsymbol{X}_{\ell m}(\hat{\boldsymbol{r}})\right). \tag{6}$$

In what follows we shall write down only the electric-field component of the wave. $j_\ell(qr)$ is the spherical Bessel function, and $\boldsymbol{X}_{\ell m}(\hat{\boldsymbol{r}})$, where the unit vector $\hat{\boldsymbol{r}}$ denotes the angular variables (θ, ϕ) of $\boldsymbol{r}$ in spherical coordinates, is a vector spherical harmonic defined by

$$\sqrt{\ell(\ell+1)}\,\boldsymbol{X}_{\ell m}(\hat{\boldsymbol{r}}) = \boldsymbol{L}Y_{\ell m}(\hat{\boldsymbol{r}}) \equiv -\mathrm{i}\boldsymbol{r}\times\nabla Y_{\ell m}(\hat{\boldsymbol{r}})\,. \tag{7}$$

$Y_{\ell m}$ denotes as usual a spherical harmonic so that for given ℓ $(=1,2,3,\ldots)$, m takes the values $-\ell, -\ell+1,\ldots,\ell-1,\ell$. By definition $\boldsymbol{X}_{00}(\hat{\boldsymbol{r}})=0$. For $\ell\geq 1$, we have

$$\begin{aligned}\sqrt{\ell(\ell+1)}\,\boldsymbol{X}_{\ell m}(\hat{\boldsymbol{r}}) = {}& \left[\alpha_\ell^m Y_{\ell m+1}(\hat{\boldsymbol{r}}) + \beta_\ell^m Y_{\ell m-1}(\hat{\boldsymbol{r}})\right]\hat{\boldsymbol{u}}_1 \\ & -\mathrm{i}\left[\alpha_\ell^m Y_{\ell m+1}(\hat{\boldsymbol{r}}) - \beta_\ell^m Y_{\ell m-1}(\hat{\boldsymbol{r}})\right]\hat{\boldsymbol{u}}_2 + mY_{\ell m}(\hat{\boldsymbol{r}})\hat{\boldsymbol{u}}_3\,,\end{aligned} \tag{8}$$

with

$$\begin{aligned}\alpha_\ell^m &\equiv \tfrac{1}{2}\left[(\ell-m)(\ell+m+1)\right]^{1/2}\,,\\ \beta_\ell^m &\equiv \tfrac{1}{2}\left[(\ell+m)(\ell-m+1)\right]^{1/2}\,,\end{aligned} \tag{9}$$

where $\hat{\boldsymbol{u}}_1$, $\hat{\boldsymbol{u}}_2$, $\hat{\boldsymbol{u}}_3$ are unit vectors on the x, y, z coordinate axes, respectively.

The coefficients $\mathrm{a}_{\ell m}^{0P}$, where $P = E, H$, in the expansions (5) and (6) of the plane wave given by Eqs. (3) and (4) can be written in the following form:

$$\mathrm{a}_{\ell m}^{0P} = \boldsymbol{A}_{\ell m}^{0P}\cdot\boldsymbol{E}_0(\boldsymbol{q})\,, \tag{10}$$

where

$$\begin{aligned}A_{\ell m,x}^{0E}(\boldsymbol{q}) &= \frac{4\pi\mathrm{i}^\ell(-1)^{m+1}}{q\sqrt{\ell(\ell+1)}}\left\{\mathrm{i}q_z\left[\alpha_\ell^m Y_{\ell-(m+1)}(\hat{\boldsymbol{q}}) - \beta_\ell^m Y_{\ell-(m-1)}(\hat{\boldsymbol{q}})\right] + mq_y Y_{\ell-m}(\hat{\boldsymbol{q}})\right\}\,,\\ A_{\ell m,y}^{0E}(\boldsymbol{q}) &= -\frac{4\pi\mathrm{i}^\ell(-1)^{m+1}}{q\sqrt{\ell(\ell+1)}}\left\{q_z\left[\alpha_\ell^m Y_{\ell-(m+1)}(\hat{\boldsymbol{q}}) + \beta_\ell^m Y_{\ell-(m-1)}(\hat{\boldsymbol{q}})\right] + mq_x Y_{\ell-m}(\hat{\boldsymbol{q}})\right\}\,,\\ A_{\ell m,z}^{0E}(\boldsymbol{q}) &= \frac{4\pi\mathrm{i}^\ell(-1)^{m+1}}{q\sqrt{\ell(\ell+1)}}\left\{(q_y-\mathrm{i}q_x)\alpha_\ell^m Y_{\ell-(m+1)}(\hat{\boldsymbol{q}}) + (q_y+\mathrm{i}q_x)\beta_\ell^m Y_{\ell-(m-1)}(\hat{\boldsymbol{q}})\right\}\,,\end{aligned}$$

and

$$\begin{aligned}A_{\ell m,x}^{0H}(\boldsymbol{q}) &= \frac{4\pi\mathrm{i}^\ell(-1)^{m+1}}{\sqrt{\ell(\ell+1)}}\left\{\alpha_\ell^m Y_{\ell-(m+1)}(\hat{\boldsymbol{q}}) + \beta_\ell^m Y_{\ell-(m-1)}(\hat{\boldsymbol{q}})\right\}\,,\\ A_{\ell m,y}^{0H}(\boldsymbol{q}) &= \frac{4\pi\mathrm{i}^\ell(-1)^{m+1}}{\sqrt{\ell(\ell+1)}}\mathrm{i}\left\{\alpha_\ell^m Y_{\ell-(m+1)}(\hat{\boldsymbol{q}}) - \beta_\ell^m Y_{\ell-(m-1)}(\hat{\boldsymbol{q}})\right\}\,,\\ A_{\ell m,z}^{0H}(\boldsymbol{q}) &= -\frac{4\pi\mathrm{i}^\ell(-1)^{m+1}}{\sqrt{\ell(\ell+1)}}mY_{\ell-m}(\hat{\boldsymbol{q}})\,.\end{aligned} \tag{11}$$

Now consider a sphere of radius S with its centre at the origin of coordinates, and assume that its relative dielectric function, $\epsilon_S(\omega)$, and/or magnetic permeability, $\mu_S(\omega)$, in general complex functions of ω, are different from those, $\epsilon(\omega)$ and $\mu(\omega)$, of the surrounding medium. When the plane wave described by Eqs. (5), (10) and (11) is incident on the sphere, it is scattered by it, so that the wavefield outside the sphere consists of the incident wave (5) and a corresponding scattered wave, which can be expanded in spherical waves as follows:

$$\boldsymbol{E}_{\mathrm{sc}}(\boldsymbol{r}) = \sum_{\ell=1}^{\infty}\sum_{m=-\ell}^{\ell}\left(\frac{\mathrm{i}}{q}\mathrm{a}_{\ell m}^{+E}\nabla\times h_\ell^+(qr)\boldsymbol{X}_{\ell m}(\hat{\boldsymbol{r}}) + \mathrm{a}_{\ell m}^{+H}h_\ell^+(qr)\boldsymbol{X}_{\ell m}(\hat{\boldsymbol{r}})\right)\,, \tag{12}$$

where $h_\ell^+(qr)$ is the spherical Hankel function, which has the asymptotic form appropriate to an outgoing spherical wave: $h_\ell^+(qr)\approx(-\mathrm{i})^\ell\exp(\mathrm{i}qr)/\mathrm{i}qr$ as $r\to\infty$. Because of the spherical symmetry of the scatterer, each spherical wave in Eq. (5) scatters independently of all others. It turns out that [7]

$$a_{\ell m}^{+,P} = T_\ell^P a_{\ell m}^{0P}, \tag{13}$$

where

$$T_\ell^E(\omega) = \left[\frac{j_\ell(q_S r)\frac{\partial}{\partial r}(r j_\ell(qr))\epsilon_S - j_\ell(qr)\frac{\partial}{\partial r}(r j_\ell(q_S r))\epsilon}{h_\ell^+(qr)\frac{\partial}{\partial r}(r j_\ell(q_S r))\epsilon - j_\ell(q_S r)\frac{\partial}{\partial r}(r h_\ell^+(qr))\epsilon_S} \right]_{r=S},$$

$$T_\ell^H(\omega) = \left[\frac{j_\ell(q_S r)\frac{\partial}{\partial r}(r j_\ell(qr))\mu_S - j_\ell(qr)\frac{\partial}{\partial r}(r j_\ell(q_S r))\mu}{h_\ell^+(qr)\frac{\partial}{\partial r}(r j_\ell(q_S r))\mu - j_\ell(q_S r)\frac{\partial}{\partial r}(r h_\ell^+(qr))\mu_S} \right]_{r=S}. \tag{14}$$

The above equations are obtained from the requirement that the tangential components of $\boldsymbol{E}$ and $\boldsymbol{H}$ be continuous at the surface of the sphere. We note that the field inside the sphere is given by Eq. (5) with the $a_{\ell m}^{0P}$ replaced by a different set of coefficients: $a_{\ell m}^{1,P}$. Given the incident wave (i.e., the coefficients $a_{\ell m}^{0P}$), the continuity of the tangential components of $\boldsymbol{E}$ and $\boldsymbol{H}$ at the surface of the sphere determines both the scattered wave (i.e., the coefficients $a_{\ell m}^{+P}$), and the wavefield inside the sphere (i.e., the coefficients $a_{\ell m}^{1,P}$). We do not need the explicit expressions for $a_{\ell m}^{1,P}$ in our calculations. We remember that the total field outside the sphere is the sum of the incident field (5) and the corresponding scattered field given by Eq. (12). It turns out that, provided that qS is not much larger than unity, a limited number of partial waves, corresponding to $\ell \le \ell_{\max}$, is sufficient for the description of the scattered field [12]. Therefore, in what follows we assume that $a_{\ell m}^{+P} = 0$ for $\ell > \ell_{\max}$. We note, however, that when multiple scattering from a plane of spheres is considered (see Section 2.2), $\ell_{\max}$ must be determined from the requirement of convergence as far as the scattering by the plane is concerned, and in this respect $\ell_{\max}$ may be greater than that obtained for scattering by a single sphere.

The subroutines relevant to this section are TMTRX, BESSEL, CNWF01, PLW and SPHRM4.

Subroutine TMTRX computes T_ℓ^E and T_ℓ^H which are stored in the arrays TE and TH, respectively, up to $\ell = \ell_{\max}$, for given ω. The program version of T_ℓ^E and T_ℓ^H follows from Eq. (14), by substituting $j_\ell + \mathrm{i}y_\ell$ for h_ℓ^+, where y_ℓ is the spherical Neumann function, and using the recurrence relation $xf_\ell'(x) = \ell f_\ell(x) - x f_{\ell+1}(x)$, $f_\ell = j_\ell$ or y_ℓ, for the first derivatives of j_ℓ and y_ℓ [13]. The spherical Bessel and Neumann functions, j_ℓ and y_ℓ, are provided by subroutine BESSEL which employs a Chebychev expansion [14] of the above functions. The expansion coefficients are computed by subroutine CNWF01.

Subroutine PLW calculates the coefficients $A_{\ell m}^{0P}$ of Eq. (11) for a given wavevector $\boldsymbol{q}$ and stores them in the arrays AE, AH. The subroutine SPHRM4 provides the spherical harmonics (YLM) contained in Eq. (11). It computes $Y_{\ell m}$ for $m = \ell, -\ell, \ell-1, -\ell+1$ and for $\ell = 1, \ldots, \ell_{\max}$ using explicit analytical expressions. Then, the remaining $Y_{\ell m}$, for given m, are obtained using the recurrence relation [13]

$$Y_{\ell+1 m}(\theta,\phi) = -\left\{ \left[\frac{(\ell+m)(\ell-m)}{(2\ell-1)(2\ell+1)} \right]^{1/2} Y_{\ell-1 m}(\theta,\phi) - \cos\theta\, Y_{\ell m}(\theta,\phi) \right\} \times \left[\frac{(2\ell+1)(2\ell+3)}{(\ell-m+1)(\ell+m+1)} \right]^{1/2}. \tag{15}$$

We note that the z component of $\boldsymbol{q}$ (denoted by q_z) can be real or imaginary. In the latter case $\cos\theta_{\boldsymbol{q}}$ in the standard formulae for $Y_{\ell m}(\hat{\boldsymbol{q}})$ is replaced by q_z/q.

2.2. Scattering by a plane of spheres

The structures we shall be dealing with may contain more than one plane of non-overlapping spheres (of the same 2D periodicity parallel to the xy-plane). To begin with, we consider just one plane, at $z = 0$, in which case the spheres are centred on the sites of a given 2D lattice specified by

$$\boldsymbol{R}_n = n_1 \boldsymbol{a}_1 + n_2 \boldsymbol{a}_2, \tag{16}$$

where $\boldsymbol{a}_1$ and $\boldsymbol{a}_2$ are primitive vectors in the xy-plane and $n_1, n_2 = 0, \pm 1, \pm 2, \pm 3, \ldots$.

We define the corresponding 2D reciprocal lattice in the usual manner [15,16] as follows:

$$\boldsymbol{g} = m_1 \boldsymbol{b}_1 + m_2 \boldsymbol{b}_2 . \tag{17}$$

where $m_1, m_2 = 0, \pm 1, \pm 2, \pm 3, \ldots$ and $\boldsymbol{b}_1, \boldsymbol{b}_2$ are defined by

$$\boldsymbol{b}_i \cdot \boldsymbol{a}_j = 2\pi \delta_{ij} . \tag{18}$$

We next construct the surface Brillouin zone (SBZ) corresponding to Eq. (17) in the usual manner [15,16]. For example, for a square lattice we have

$$\begin{aligned} &\boldsymbol{a}_1 = a\hat{u}_1 , \qquad \boldsymbol{a}_2 = a\hat{u}_2 , \\ &\boldsymbol{b}_1 = (2\pi/a)\hat{u}_1 , \qquad \boldsymbol{b}_2 = (2\pi/a)\hat{u}_2 , \end{aligned} \tag{19}$$

and the SBZ is a square in reciprocal space.

Let the plane wave, described by Eqs. (3) and (4), be incident on the plane of spheres. We can always write the component of its wavevector parallel to the plane of spheres as follows:

$$\boldsymbol{q}_{\parallel} = \boldsymbol{k}_{\parallel} + \boldsymbol{g}' , \tag{20}$$

where the reduced wavevector $\boldsymbol{k}_{\parallel}$ lies in the SBZ and $\boldsymbol{g}'$ is one of the reciprocal-lattice vectors (17). A special subroutine has been constructed which implements Eq. (20) for a given 2D lattice (oblique, centred rectangular, rectangular, square and hexagonal). We note that according to Eqs. (17), (18) and (20), $\exp(i\boldsymbol{q}_{\parallel} \cdot \boldsymbol{R}_n) = \exp(i\boldsymbol{k}_{\parallel} \cdot \boldsymbol{R}_n)$.

In what follows we shall write the wavevector of a plane wave of given $q = \sqrt{\mu\epsilon}\,\omega/c$ and given $\boldsymbol{q}_{\parallel} = \boldsymbol{k}_{\parallel} + \boldsymbol{g}$ as follows:

$$\boldsymbol{K}_{\boldsymbol{g}}^{\pm} = \left(\boldsymbol{k}_{\parallel} + \boldsymbol{g}, \pm \left[q^2 - \left(\boldsymbol{k}_{\parallel} + \boldsymbol{g} \right)^2 \right]^{1/2} \right) , \tag{21}$$

where the $+,-$ sign defines the sign of the z-component of the wavevector. We note that when $q^2 < (\boldsymbol{k}_{\parallel} + \boldsymbol{g})^2$, the above defines a decaying wave, so that the positive sign in Eq. (21) describes a wave propagating or decaying to the right and the negative sign describes a wave propagating or decaying to the left.

Let the electric field of an incident on the plane of spheres wave be described by

$$\boldsymbol{E}_{\mathrm{in}}^{s}(\boldsymbol{r}) = \sum_{i=1}^{3} [E_{\mathrm{in}}]_{\boldsymbol{g}'i}^{s} \exp(i\boldsymbol{K}_{\boldsymbol{g}'}^{s} \cdot \boldsymbol{r}) \hat{u}_i , \tag{22}$$

where $s = +(-)$ corresponds to a propagating or decaying wave incident on the plane of spheres from the left (right).

Because of the 2D periodicity of the structure under consideration, the scattered wave corresponding to the incident wave (22) can be written in the following form:

$$\begin{aligned} \boldsymbol{E}_{\mathrm{sc}}(\boldsymbol{r}) = \sum_{l=1}^{\infty} \sum_{m=-l}^{l} \Bigg(& \frac{\mathrm{i}}{q} \mathrm{b}_{lm}^{sE} \nabla \times \sum_{\boldsymbol{R}_n} \exp(i\boldsymbol{k}_{\parallel} \cdot \boldsymbol{R}_n) h_l^{-}(qr_n) \boldsymbol{X}_{lm}(\hat{\boldsymbol{r}}_n) \\ & + \mathrm{b}_{lm}^{sH} \sum_{\boldsymbol{R}_n} \exp(i\boldsymbol{k}_{\parallel} \cdot \boldsymbol{R}_n) h_l^{-}(qr_n) \boldsymbol{X}_{lm}(\hat{\boldsymbol{r}}_n) \Bigg) , \end{aligned} \tag{23}$$

where $\boldsymbol{r}_n = \boldsymbol{r} - \boldsymbol{R}_n$. Eq. (23) tells us that the scattered wave is a sum of outgoing spherical waves centred on the spheres of the plane, and that the wave scattered from the sphere at $\boldsymbol{R}_n$ differs from that scattered from the sphere at the origin ($\boldsymbol{R}_n = 0$) only by the phase factor $\exp(\mathrm{i}\boldsymbol{k}_\parallel \cdot \boldsymbol{R}_n)$.

Now the coefficients $b_{\ell m}^{+P}$ which determine the scattered wave from the sphere at the origin are determined from the *total* incident wave on that sphere, which consists of the incident plane wave and the waves scattered from all the other spheres described by the terms corresponding to $\boldsymbol{R}_n \neq 0$ in Eq. (23). The latter can be expanded into spherical waves about the origin; we have

$$\boldsymbol{E}'_{\mathrm{sc}}(\boldsymbol{r}) = \sum_{\ell=1}^{\infty} \sum_{m=-\ell}^{\ell} \left(\frac{\mathrm{i}}{q} \mathrm{b}'^{E}_{\ell m} \nabla \times j_\ell(qr) \boldsymbol{X}_{\ell m}(\hat{\boldsymbol{r}}) + \mathrm{b}'^{H}_{\ell m} j_\ell(qr) \boldsymbol{X}_{\ell m}(\hat{\boldsymbol{r}}) \right), \tag{24}$$

where $\boldsymbol{E}'_{\mathrm{sc}}(\boldsymbol{r})$ is obtained from $\boldsymbol{E}_{\mathrm{sc}}(\boldsymbol{r})$ omitting the term corresponding to $\boldsymbol{R}_n = 0$ in the sum of Eq. (23). It can be shown that [7]

$$b'^{P}_{\ell m} = \sum_{P'=E,H} \sum_{\ell'=1}^{\infty} \sum_{m'=-\ell'}^{\ell'} \Omega^{PP'}_{\ell m,\ell' m'} b^{+P'}_{\ell' m'}, \tag{25}$$

where

$$\begin{aligned}
\Omega^{EE}_{\ell m;\ell' m'} &= \left[\ell(\ell+1)\ell'(\ell'+1)\right]^{-1/2} \left(2\beta_\ell^m \beta_{\ell'}^{m'} Z_{\ell m-1;\ell' m'-1} + 2\alpha_\ell^m \alpha_{\ell'}^{m'} Z_{\ell m+1,\ell' m'+1} + m m' Z_{\ell m;\ell' m'} \right), \\
\Omega^{EH}_{\ell m;\ell' m'} &= \left[\ell(\ell+1)\ell'(\ell'+1)\right]^{-1/2} (2\ell+1)\{(8\pi/3)^{1/2}(-1)^m \\
&\quad \times \alpha_{\ell'}^{m'} Z_{\ell m+1,\ell'-1,m'+1} B_{\ell-1,m+1}(1,-1;\ell m) - (8\pi/3)^{1/2}(-1)^m \\
&\quad \times \beta_{\ell'}^{m'} Z_{\ell m-1;\ell'-1,m'-1} B_{\ell-1,m-1}(1,1;\ell m) + m' Z_{\ell m;\ell'-1 m'} \\
&\quad \times \left[(\ell+m)(\ell-m)/(2\ell-1)(2\ell+1)\right]^{1/2}\}, \\
\Omega^{HH}_{\ell m;\ell' m'} &= \Omega^{EE}_{\ell m,\ell' m'}, \\
\Omega^{HE}_{\ell m;\ell' m'} &= -\Omega^{EH}_{\ell m,\ell' m'},
\end{aligned} \tag{26}$$

where α_ℓ^m and β_ℓ^m are given by Eq. (9) and

$$Z_{\ell m;\ell' m'} \equiv \sum_{\boldsymbol{R}_n \neq 0} \exp(\mathrm{i}\boldsymbol{k}_\parallel \cdot \boldsymbol{R}_n) G_{\ell m;\ell' m'}(-\boldsymbol{R}_n), \tag{27}$$

with

$$G_{\ell m;\ell' m'}(-\boldsymbol{R}_n) \equiv \sum_{\ell''=0}^{\infty} \sum_{m''=-\ell''}^{\ell''} E_{\ell' m'}(\ell'' m'';\ell m) h^+_{\ell''}(qR_n) Y_{\ell''-m''}(-\hat{\boldsymbol{R}}_n), \tag{28}$$

$$E_{\ell' m'}(\ell'' m'';\ell m) \equiv 4\pi(-1)^{(\ell'-\ell-\ell'')/2}(-1)^{m+m''} B_{\ell' m'}(\ell'' m'';\ell m), \tag{29}$$

$$B_{\ell' m'}(\ell'' m'';\ell m) \equiv \int \mathrm{d}\hat{\boldsymbol{r}}\, Y_{\ell'-m'}(\hat{\boldsymbol{r}}) Y_{\ell'' m''}(\hat{\boldsymbol{r}}) Y_{\ell m}(\hat{\boldsymbol{r}}). \tag{30}$$

We see that the evaluation of the matrices $\boldsymbol{\Omega}^{PP'}$ involves the evaluation of the matrix $\mathbf{Z}$ defined by Eq. (27). The latter matrix is a well-known quantity in the theory of low-energy electron diffraction (LEED) and a computer program for its evaluation is already available in the literature [15]. Further calculation is made simpler by the following property of $Z_{\ell m,\ell' m'}$ [15]:

$$Z_{\ell m;\ell' m'} = 0 \begin{cases} \text{unless } \ell + m \text{ even and } \ell' + m' \text{ even,} \\ \text{or } \ell + m \text{ odd and } \ell' + m' \text{ odd.} \end{cases} \tag{31}$$

It follows from Eq. (31) that

$$\Omega^{EE}_{\ell m;\ell' m'} = 0 \begin{cases} \text{unless } \ell + m \text{ even and } \ell' + m' \text{ even,} \\ \text{or } \ell + m \text{ odd and } \ell' + m' \text{ odd,} \end{cases}$$

$$\Omega^{EH}_{\ell m;\ell' m'} = 0 \begin{cases} \text{unless } \ell + m \text{ even and } \ell' + m' \text{ odd,} \\ \text{or } \ell + m \text{ odd and } \ell' + m' \text{ even.} \end{cases} \tag{32}$$

Finally, it is convenient to write Eq. (25) in a more compact form. In a practical calculation there will be a finite number of partial waves contributing to the EM field corresponding to $\ell_{\max}(\ell_{\max}+2)$ values of (ℓ, m) which we order in a specific manner, as follows: $(1,-1)$, $(1,0)$, $(1,1)$, $(2,-2)$, $(2,-1)$, ... We can then write Eq. (25) in matrix form,

$$\begin{pmatrix} \boldsymbol{b}'^{E} \\ \boldsymbol{b}'^{H} \end{pmatrix} = \begin{pmatrix} \boldsymbol{\Omega}^{EE} & \boldsymbol{\Omega}^{EH} \\ \boldsymbol{\Omega}^{HE} & \boldsymbol{\Omega}^{HH} \end{pmatrix} \begin{pmatrix} \boldsymbol{b}^{+E} \\ \boldsymbol{b}^{+H} \end{pmatrix}, \tag{33}$$

where $\boldsymbol{b}'^{P} \equiv \{b'^{P}_{\ell m}\}$ are column matrices of $\ell_{\max}(\ell_{\max}+2)$ elements and $\boldsymbol{\Omega}^{PP'}$ are $\ell_{\max}(\ell_{\max}+2) \times \ell_{\max}(\ell_{\max}+2)$ matrices. It is worth noting that $\boldsymbol{\Omega}^{PP'}$ depend on the geometry (16) of the plane and, through q, on the frequency and on the dielectric function of the medium surrounding the spheres of the plane; they depend also on the reduced wavevector $\boldsymbol{k}_{\|}$ of the incident light; but they do not depend on the scattering properties of the individual sphere.

The latter enter the determination of $\boldsymbol{b}^{+P} = \{b^{+P}_{\ell m}\}$, which describe the scattered wave from the sphere at the origin of the coordinates as follows:

$$\begin{pmatrix} \boldsymbol{b}^{+E} \\ \boldsymbol{b}^{+H} \end{pmatrix} = \begin{pmatrix} \mathbf{T}^{E} & \mathbf{0} \\ \mathbf{0} & \mathbf{T}^{H} \end{pmatrix} \begin{pmatrix} \boldsymbol{a}^{0E} + \boldsymbol{b}'^{E} \\ \boldsymbol{a}^{0H} + \boldsymbol{b}'^{H} \end{pmatrix}, \tag{34}$$

where $\mathbf{0}$ is the $\ell_{\max}(\ell_{\max}+2) \times \ell_{\max}(\ell_{\max}+2)$ zero matrix and $\mathbf{T}^{P}$, $P = E, H$, are the $\ell_{\max}(\ell_{\max}+2) \times \ell_{\max}(\ell_{\max}+2)$ diagonal matrices

$$T^{P}_{\ell m;\ell' m'} = T^{P}_{\ell} \delta_{\ell\ell'} \delta_{mm'}, \tag{35}$$

which describe the scattering of light by an individual sphere according to Eq. (14). The column matrix on the right-hand side of Eq. (34) represents the total wave incident on the sphere at the origin of coordinates; $\boldsymbol{a}^{0P} \equiv \{a^{0P}_{\ell m}\}$ derives from the incident plane wave (22) according to Eqs. (10) and (11), and $\boldsymbol{b}'^{P}$ from the field defined by Eq. (24). Combining Eqs. (33) and (34), we obtain

$$\begin{pmatrix} \mathbf{I} - \mathbf{T}^{E}\boldsymbol{\Omega}^{EE} & \mathbf{T}^{E}\boldsymbol{\Omega}^{EH} \\ \mathbf{T}^{H}\boldsymbol{\Omega}^{HE} & \mathbf{I} - \mathbf{T}^{H}\boldsymbol{\Omega}^{HH} \end{pmatrix} \begin{pmatrix} \boldsymbol{b}^{+E} \\ \boldsymbol{b}^{+H} \end{pmatrix} = \begin{pmatrix} \mathbf{T}^{E}\boldsymbol{a}^{0E} \\ \mathbf{T}^{H}\boldsymbol{a}^{0H} \end{pmatrix}, \tag{36}$$

where $\mathbf{I}$ is the $\ell_{\max}(\ell_{\max}+2) \times \ell_{\max}(\ell_{\max}+2)$ unit matrix. Eq. (36) gives the coefficients $b^{+P}_{\ell m}$ in the expression (23) for the wave scattered from the plane of spheres in terms of the coefficients $a^{0P}_{\ell m}$ of the incident wave.

Finally, the scattered wave (23) can be expressed as a sum of plane waves using the following formula:

$$\sum_{\boldsymbol{R}_n} \exp(\mathrm{i}\boldsymbol{k}_{\|} \cdot \boldsymbol{R}_n) h^{+}_{\ell}(qr_n) Y_{\ell m}(\hat{\boldsymbol{r}}_n) = \sum_{\boldsymbol{g}} \frac{2\pi(\mathrm{i})^{-\ell}}{qA_0 K^{\pm}_{\boldsymbol{g}z}} Y_{\ell m}(\hat{\boldsymbol{K}}^{\pm}_{\boldsymbol{g}}) \exp(\mathrm{i}\boldsymbol{K}^{\pm}_{\boldsymbol{g}} \cdot \boldsymbol{r}), \tag{37}$$

where A_0 denotes the area of the unit cell of the lattice (16) and $\boldsymbol{K}_{\boldsymbol{g}}^{\pm}$ are given by Eq. (21). The plus (minus) sign on $\boldsymbol{K}_{\boldsymbol{g}}$ must be used for $z > 0$ ($z < 0$). We note that the z-component of $\boldsymbol{K}_{\boldsymbol{g}}^{\pm}$ (denoted by $K_{gz}^{\pm}$) can be real or imaginary. In the latter case $\cos\theta_{\boldsymbol{K}_{\boldsymbol{g}}^{\pm}}$ in the standard formulae for $Y_{\ell m}(\hat{\boldsymbol{K}}_{\boldsymbol{g}}^{\pm})$ is replaced by $K_{gz}^{\pm}/q$.

Using Eq. (37) we can write the scattered wave (23) as follows:

$$\boldsymbol{E}_{\mathrm{sc}}^{s}(\boldsymbol{r}) = \sum_{i=1}^{3}\sum_{\boldsymbol{g}} [E_{\mathrm{sc}}]_{\boldsymbol{g}i}^{s} \exp(\mathrm{i}\boldsymbol{K}_{\boldsymbol{g}}^{s}\cdot\boldsymbol{r})\hat{u}_i\,, \tag{38}$$

where the superscript $s = +(-)$ holds for $z > 0$ ($z < 0$). $\boldsymbol{K}_{\boldsymbol{g}}^{\pm}$ are given by Eq. (21); they have the same magnitude q and the same reduced wavevector $\boldsymbol{k}_{\parallel}$ as the incident wave. We see that the scattered wave consists, in general, of a number of diffracted beams corresponding to different $\boldsymbol{g}$-vectors. We note, however, that only beams for which $K_{gz}^{\pm}$ is real constitute propagating waves. The coefficients in Eq. (38) are, of course, functions of the $b_{\ell m}^{+P}$-coefficients and through them depend on the incident plane wave. In what follows we shall write $b_{\ell m}^{+P}(s', \boldsymbol{g}', i')$ instead of $b_{\ell m}^{+P}$ to indicate that this quantity is to be evaluated for an incident plane wave with parallel wavevector $\boldsymbol{k}_{\parallel} + \boldsymbol{g}'$, incident from the left (right) corresponding to $s' = +(-)$, with an electric field, along the i'th direction, of magnitude equal to unity. In other words, $b_{\ell m}^{+P}(s', \boldsymbol{g}', i')$ are calculated from Eq. (36), substituting $A_{\ell m,i'}^{0P}(\boldsymbol{K}_{\boldsymbol{g}'}^{s'})$ (see Eqs. (10) and (11)) for $a_{\ell m}^{0P}(s', \boldsymbol{g}', i')$ in the right-hand side of Eq. (36).

Let us for the sake of clarity assume that a plane wave (22) is incident on the plane of spheres from the left as in Fig. 1a. Then the transmitted wave (incident+scattered) on the right of the plane of spheres can be written as

$$\boldsymbol{E}_{\mathrm{tr}}^{+}(\boldsymbol{r}) = \sum_{i=1}^{3}\sum_{\boldsymbol{g}} [E_{\mathrm{tr}}]_{\boldsymbol{g}i}^{+} \exp(\mathrm{i}\boldsymbol{K}_{\boldsymbol{g}}^{+}\cdot\boldsymbol{r})\hat{u}_i\,, \quad z > 0\,, \tag{39}$$

with

$$[E_{\mathrm{tr}}]_{\boldsymbol{g}i}^{+} = [E_{\mathrm{in}}]_{\boldsymbol{g}'i}^{+}\delta_{\boldsymbol{g}\boldsymbol{g}'} + [E_{\mathrm{sc}}]_{\boldsymbol{g}i}^{+} = \sum_{i'} M_{\boldsymbol{g}i;\boldsymbol{g}'i'}^{++}[E_{\mathrm{in}}]_{\boldsymbol{g}'i'}^{+} \tag{40}$$

and the reflected wave as

$$\boldsymbol{E}_{\mathrm{rf}}^{-}(\boldsymbol{r}) = \sum_{i=1}^{3}\sum_{\boldsymbol{g}} [E_{\mathrm{rf}}]_{\boldsymbol{g}i}^{-} \exp(\mathrm{i}\boldsymbol{K}_{\boldsymbol{g}}^{-}\cdot\boldsymbol{r})\hat{u}_i\,, \quad z < 0\,, \tag{41}$$

with

$$[E_{\mathrm{rf}}]_{\boldsymbol{g}i}^{-} = [E_{\mathrm{sc}}]_{\boldsymbol{g}i}^{-} = \sum_{i'} M_{\boldsymbol{g}i;\boldsymbol{g}'i'}^{-+}[E_{\mathrm{in}}]_{\boldsymbol{g}'i'}^{+}\,. \tag{42}$$

Similarly, we can define the transmission matrix elements $M_{\boldsymbol{g}i;\boldsymbol{g}'i'}^{--}$ and the reflection matrix elements $M_{\boldsymbol{g}i;\boldsymbol{g}'i'}^{+-}$ starting from a plane wave incident on the plane of spheres from the right (see Fig. 1b). The M-matrix elements are

$$M_{\boldsymbol{g}i;\boldsymbol{g}'i'}^{ss'} = \delta_{ss'}\delta_{\boldsymbol{g}\boldsymbol{g}'}\delta_{ii'} + \sum_{P=E,H}\sum_{\ell=1}^{\infty}\sum_{m=-\ell}^{\ell}\Delta_{\ell m,i}^{P}(\boldsymbol{K}_{\boldsymbol{g}}^{s})b_{\ell m}^{s'P}(s', \boldsymbol{g}', i')\,, \tag{43}$$

where

$$\Delta_{\ell m}^{H}(\boldsymbol{K}_{\boldsymbol{g}}^{s}) = \frac{2\pi(-\mathrm{i})^{\ell}}{qA_0K_{gz}^{s}}X_{\ell m}(\hat{\boldsymbol{K}}_{\boldsymbol{g}}^{s})\,,$$

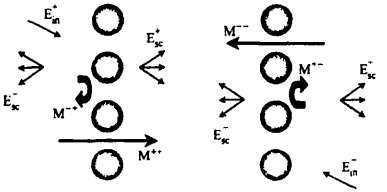

Fig. 1. Scattering of a plane EM wave from a plane of spheres: (a) plane wave incident from the left; (b) plane wave incident from the right.

$$\Delta^{E}_{lm}(\boldsymbol{K}^{\lambda}_{g}) = -\frac{\boldsymbol{K}^{\lambda}_{g}}{q} \times \Delta^{H}_{lm}(\boldsymbol{K}^{\lambda}_{g}) , \tag{44}$$

where $\boldsymbol{X}_{lm}$ are the vector spherical harmonics of Eq. (8). One can easily show that the **M**-matrix elements obey the following symmetry relations:

$$M^{-\lambda-\lambda'}_{g_l;g'_{l'}} = M^{\lambda\lambda'}_{g_l;g'_{l'}} \quad \text{for } (i,i') = (x,x),(y,y),(z,z),(x,y),(y,x),$$
$$M^{-\lambda-\lambda'}_{g_l;g'_{l'}} = -M^{\lambda\lambda'}_{g_l;g'_{l'}} \quad \text{for } (i,i') = (x,z),(z,x),(y,z),(z,y). \tag{45}$$

The more general structure that can be dealt with by our program consists of elements which can be either planes of spheres or homogeneous plates (see Section 1). These can be incorporated into the program by treating formally each plate as another element characterized by appropriate scattering matrices (see Section 2.3). In any case we shall need to evaluate the scattering properties of a slice which by definition consists of a number of elements (an element being either a plane of spheres or a homogeneous plate). For this purpose it is convenient to express the waves on the left of a given plane of spheres with respect to an origin, $\boldsymbol{A}_l$, on the left of the plane at $-\boldsymbol{d}_l$ from its centre and the waves on the right of this plane with respect to an origin, $\boldsymbol{A}_r$, on the right of the plane at $\boldsymbol{d}_r$ from its centre, i.e. a plane wave on the left of the plane will be written as $\boldsymbol{E}^{\lambda}_{g}\exp(\mathrm{i}\boldsymbol{K}^{\lambda}_{g}\cdot(\boldsymbol{r}-\boldsymbol{A}_l))$ and a wave on the right of the plane will be written as $\boldsymbol{E}^{\lambda}_{g}\exp(\mathrm{i}\boldsymbol{K}^{\lambda}_{g}\cdot(\boldsymbol{r}-\boldsymbol{A}_r))$. With the above choice of origins the transmission/reflection matrix elements of a plane of spheres become

$$Q^{\mathrm{I}}_{g_l;g'_{l'}} = M^{++}_{g_l;g'_{l'}}\exp\left(\mathrm{i}(\boldsymbol{K}^{+}_{g}\cdot\boldsymbol{d}_r + \boldsymbol{K}^{+}_{g'}\cdot\boldsymbol{d}_l)\right) ,$$
$$Q^{\mathrm{II}}_{g_l;g'_{l'}} = M^{+-}_{g_l;g'_{l'}}\exp\left(\mathrm{i}(\boldsymbol{K}^{+}_{g}\cdot\boldsymbol{d}_r - \boldsymbol{K}^{-}_{g'}\cdot\boldsymbol{d}_r)\right) ,$$
$$Q^{\mathrm{III}}_{g_l;g'_{l'}} = M^{-+}_{g_l;g'_{l'}}\exp\left(-\mathrm{i}(\boldsymbol{K}^{-}_{g}\cdot\boldsymbol{d}_l - \boldsymbol{K}^{+}_{g'}\cdot\boldsymbol{d}_l)\right) ,$$
$$Q^{\mathrm{IV}}_{g_l;g'_{l'}} = M^{--}_{g_l;g'_{l'}}\exp\left(-\mathrm{i}(\boldsymbol{K}^{-}_{g}\cdot\boldsymbol{d}_l + \boldsymbol{K}^{-}_{g'}\cdot\boldsymbol{d}_r)\right) . \tag{46}$$

In what follows we shall write the above matrix elements in compact form as follows: $\mathbf{Q}^{\mathrm{I}}$, $\mathbf{Q}^{\mathrm{II}}$, $\mathbf{Q}^{\mathrm{III}}$, and $\mathbf{Q}^{\mathrm{IV}}$ which implies a definite sequence in the ordering of the indices: g_1x, g_1y, g_1z, g_2x, g_2y, g_2z, ...

The main subroutines relevant to this section are LAT2D, REDUCE, and PCSLAB.

With input the primitive vectors of a 2D lattice (in real or reciprocal space) and a positive parameter RMAX, subroutine LAT2D calculates all lattice vectors (their number equals IMAX) which have a magnitude (VECMOD) less than RMAX. LAT2D is called in the main program in order to find the set of IGMAX reciprocal-lattice vectors of Eq. (17) which are stored in array G.

Subroutine REDUCE takes as input $\boldsymbol{q}_{\|}$ (stored in the array AK), the reciprocal-lattice vectors, $\boldsymbol{g}$, and the primitive vectors, $\boldsymbol{a}_1$, $\boldsymbol{a}_2$, of the 2D lattice of Eq. (16), in order to reduce the input $\boldsymbol{q}_{\|}$ to a wavevector within the corresponding SBZ in the manner of Eq. (20). First, REDUCE calculates the coordinates of the vertices of the SBZ. Then, one by one, the reciprocal-lattice vectors found by LAT2D are subtracted from $\boldsymbol{q}_{\|}$, until for one such vector, $\boldsymbol{g}'$, the reduced wavevector, $\boldsymbol{q}_{\|} - \boldsymbol{g}'$, lies within the SBZ. If none of the available reciprocal-lattice vectors reduces $\boldsymbol{q}_{\|}$, the program run stops and the user must enter a greater value for RMAX. The subroutine returns the reduced wavevector $\boldsymbol{k}_{\|}(= \boldsymbol{q}_{\|} - \boldsymbol{g}')$ in the array AK and saves in the variable IG0 the index of the appropriate reciprocal-lattice vector, $\boldsymbol{g}'$.

Subroutine PCSLAB is the main subroutine of the program and computes the matrix elements of $\mathbf{Q}$, according to Eqs. (43) and (46). It will be discussed thoroughly in Section 3.

2.3. Scattering by a homogeneous plate

We consider a homogeneous plate of thickness d, characterized by a generally complex dielectric function $\epsilon_2(\omega)\epsilon_0$ and a magnetic permeability $\mu_2(\omega)\mu_0$, sandwiched between a homogeneous medium of real $\epsilon_1(\omega)$ and $\mu_1(\omega)$ on the left (extending to $-\infty$) and a homogeneous medium of real $\epsilon_3(\omega)$ and $\mu_3(\omega)$ on the right (extending to $+\infty$). Putting the left interface at $z = 0$ and the right interface at $z = d$, we refer (to begin with) the waves on the left of the plate to an origin $\boldsymbol{A}_0 = (0,0,0)$ and the waves on its right to an origin $\boldsymbol{A}_d = (0,0,d)$. For example, a plane wave incident on the plate from the left will be written as

$$\boldsymbol{E}_{\mathrm{in}}^{+}(\boldsymbol{r}) = \sum_{i=1}^{3} [E_{\mathrm{in}}]_i^{+} \exp(\mathrm{i}\boldsymbol{q}_1^{+} \cdot (\boldsymbol{r} - \boldsymbol{A}_0))\hat{u}_i \tag{47}$$

and the corresponding transmitted and reflected waves will be written as

$$\boldsymbol{E}_{\mathrm{tr}}^{+}(\boldsymbol{r}) = \sum_{i=1}^{3} [E_{\mathrm{tr}}]_i^{+} \exp(\mathrm{i}\boldsymbol{q}_3^{+} \cdot (\boldsymbol{r} - \boldsymbol{A}_d))\hat{u}_i \tag{48}$$

and

$$\boldsymbol{E}_{\mathrm{rf}}^{-}(\boldsymbol{r}) = \sum_{i=1}^{3} [E_{\mathrm{rf}}]_i^{-} \exp(\mathrm{i}\boldsymbol{q}_1^{-} \cdot (\boldsymbol{r} - \boldsymbol{A}_0))\hat{u}_i , \tag{49}$$

respectively, where $\boldsymbol{q}_j^{\pm} = \left(\boldsymbol{q}_{\|}, \pm q_{jz}\right)$, with $q_{jz} = (\mu_j\epsilon_j\omega^2/c^2 - \boldsymbol{q}_{\|}^2)^{1/2}$. The coefficients in the expansions (48) and (49) are related to those of the incident wave (47) by the equations

$$[E_{\mathrm{tr}}]_i^{s} = \sum_{i'=1}^{3} N_{ii'}^{ss'} [E_{\mathrm{in}}]_{i'}^{s'} , \tag{50}$$

$$[E_{\mathrm{rf}}]_i^{-s} = \sum_{i'=1}^{3} N_{ii'}^{-ss'} [E_{\mathrm{in}}]_{i'}^{s'} , \tag{51}$$

where the $s = +(-)$ sign denotes a wave propagating to the right (left). The matrices $\mathbf{N}^{ss'}$, for given ω and $\boldsymbol{q}_{\|}$, have the form

$$N_{ii'}^{ss'} = \begin{pmatrix} N_x^{ss'}\cos^2\phi + N_y^{ss'}\sin^2\phi & (N_x^{ss'} - N_y^{ss'})\sin\phi\cos\phi & 0 \\ (N_x^{ss'} - N_y^{ss'})\sin\phi\cos\phi & N_x^{ss'}\sin^2\phi + N_y^{ss'}\cos^2\phi & 0 \\ 0 & 0 & N_z^{ss'} \end{pmatrix}, \tag{52}$$

where we denote by ϕ the azimuthal angle of $\boldsymbol{q}_\parallel$ with respect to the x-axis. $N_i^{ss'}$ are given by

$$
\begin{aligned}
N_i^{++} &= T_i^{(2,3)} T_i^{(1,2)} \exp(\mathrm{i}q_{2z}d) \left[1 - \exp(\mathrm{i}2q_{2z}d) R_i^{(2,1)} R_i^{(2,3)}\right]^{-1}, \\
N_i^{+-} &= R_i^{(3,2)} + T_i^{(2,3)} R_i^{(2,1)} T_i^{(3,2)} \exp(\mathrm{i}2q_{2z}d) \left[1 - \exp(\mathrm{i}2q_{2z}d) R_i^{(2,1)} R_i^{(2,3)}\right]^{-1}, \\
N_i^{-+} &= R_i^{(1,2)} + T_i^{(2,1)} R_i^{(2,3)} T_i^{(1,2)} \exp(\mathrm{i}2q_{2z}d) \left[1 - \exp(\mathrm{i}2q_{2z}d) R_i^{(2,1)} R_i^{(2,3)}\right]^{-1}, \\
N_i^{--} &= T_i^{(2,1)} T_i^{(3,2)} \exp(\mathrm{i}q_{2z}d) \left[1 - \exp(\mathrm{i}2q_{2z}d) R_i^{(2,1)} R_i^{(2,3)}\right]^{-1},
\end{aligned}
\tag{53}
$$

for $i = x, y, z$, where

$$
\begin{aligned}
R_x^{(j,j')} &= \frac{\mu_j \epsilon_j q_{j'z} - \mu_{j'} \epsilon_{j'} q_{jz}}{\mu_j \epsilon_j q_{j'z} + \mu_{j'} \epsilon_{j'} q_{jz}}, \qquad T_x^{(j,j')} = \frac{2\mu_j \epsilon_j q_{j'z}}{\mu_j \epsilon_j q_{j'z} + \mu_{j'} \epsilon_{j'} q_{jz}}, \\
R_y^{(j,j')} &= \frac{q_{jz} - q_{j'z}}{q_{jz} + q_{j'z}}, \qquad T_y^{(j,j')} = \frac{2q_{jz}}{q_{jz} + q_{j'z}} \\
R_z^{(j,j')} &= \frac{\mu_{j'} \epsilon_{j'} q_{jz} - \mu_j \epsilon_j q_{j'z}}{\mu_j \epsilon_j q_{j'z} + \mu_{j'} \epsilon_{j'} q_{jz}}, \qquad T_z^{(j,j')} = \frac{2\mu_j \epsilon_j q_{jz}}{\mu_j \epsilon_j q_{j'z} + \mu_{j'} \epsilon_{j'} q_{jz}},
\end{aligned}
\tag{54}
$$

with $(j, j') = (1,2), (2,1), (2,3), (3,2)$.

In the structures we shall be dealing with, the homogeneous plate constitutes a component of a unit slice which contains planes of spheres of given 2D periodicity (see Section 1) and, therefore, the parallel component of the wavevector has the form $\boldsymbol{q}_\parallel = \boldsymbol{k}_\parallel + \boldsymbol{g}$, where $\boldsymbol{g}$ may be any one of a number of reciprocal-lattice vectors (17).

Finally we express the waves on the left (right) of the plate with respect to an origin at $-\boldsymbol{d}_l$ ($\boldsymbol{d}_r$) from $\boldsymbol{A}_0$ ($\boldsymbol{A}_d$), for the same reasons as those given for the derivation of Eqs. (46). Referred to the new origins, the transmission/reflection matrix elements of the homogeneous plate become

$$
\begin{aligned}
Q^{\mathrm{I}}_{\boldsymbol{g}i;\boldsymbol{g}'i'} &= \delta_{\boldsymbol{g}\boldsymbol{g}'} N_{ii'}^{++} \exp\left(\mathrm{i}(\boldsymbol{K}_{3\boldsymbol{g}}^{+} \cdot \boldsymbol{d}_r + \boldsymbol{K}_{1\boldsymbol{g}'}^{+} \cdot \boldsymbol{d}_l)\right), \\
Q^{\mathrm{II}}_{\boldsymbol{g}i;\boldsymbol{g}'i'} &= \delta_{\boldsymbol{g}\boldsymbol{g}'} N_{ii'}^{+-} \exp\left(\mathrm{i}(\boldsymbol{K}_{3\boldsymbol{g}}^{+} \cdot \boldsymbol{d}_r - \boldsymbol{K}_{3\boldsymbol{g}'}^{-} \cdot \boldsymbol{d}_r)\right), \\
Q^{\mathrm{III}}_{\boldsymbol{g}i;\boldsymbol{g}'i'} &= \delta_{\boldsymbol{g}\boldsymbol{g}'} N_{ii'}^{-+} \exp\left(-\mathrm{i}(\boldsymbol{K}_{1\boldsymbol{g}}^{-} \cdot \boldsymbol{d}_l - \boldsymbol{K}_{1\boldsymbol{g}'}^{+} \cdot \boldsymbol{d}_l)\right), \\
Q^{\mathrm{IV}}_{\boldsymbol{g}i;\boldsymbol{g}'i'} &= \delta_{\boldsymbol{g}\boldsymbol{g}'} N_{ii'}^{--} \exp\left(-\mathrm{i}(\boldsymbol{K}_{1\boldsymbol{g}}^{-} \cdot \boldsymbol{d}_l + \boldsymbol{K}_{3\boldsymbol{g}'}^{-} \cdot \boldsymbol{d}_r)\right),
\end{aligned}
\tag{55}
$$

where

$$
\boldsymbol{K}_{j\boldsymbol{g}}^{\pm} = \left(\boldsymbol{k}_\parallel + \boldsymbol{g}, \pm \left[\mu_j \epsilon_j \omega^2/c^2 - (\boldsymbol{k}_\parallel + \boldsymbol{g})^2\right]^{1/2}\right). \tag{56}
$$

We note that Eqs. (55) remain valid when $d = 0$, in which case they describe the transmission/reflection at the interface between two media characterized by $\epsilon_1(\omega)$, $\mu_1(\omega)$, and $\epsilon_3(\omega)$, $\mu_3(\omega)$, respectively. In this case the input values of $\epsilon_2(\omega)$ and $\mu_2(\omega)$ are irrelevant.

The subroutine relevant to this section is HOSLAB. This implements Eqs. (52)–(55) and returns the appropriate matrix elements of **Q**, given by Eq. (55). For $d = 0$ the same subroutine provides the **Q**-matrices for an interface between two homogeneous media.

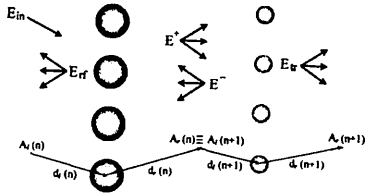

Fig. 2.

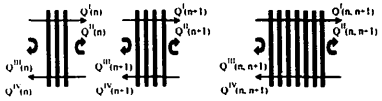

Fig. 3.

Fig. 2. Scattering from a pair of planes of spheres.

Fig. 3. The Q-matrices for two successive elements are obtained from those of the individual elements.

2.4. *Scattering by a slice*

A slice consists of a finite number of elements, where an element may be a plane of spheres as defined in Section 2.2, or a homogeneous plate as defined in Section 2.3. We note that if two successive planes of spheres lie in different host materials, separated by an interface, the interface is treated formally as a scattering element, as explained in Section 2.3. We should point out that the choice of $\boldsymbol{d}_l(n)$ and $\boldsymbol{d}_r(n)$ for the nth element is to some degree arbitrary, but it must be such that the origins of expansion of the wavefields, $\boldsymbol{A}_r(n)$ and $\boldsymbol{A}_l(n+1)$, between the successive elements, n and $n+1$, coincide (see Fig. 2).

We obtain the transmission and reflection matrices of two successive elements, n and $n+1$, by combining the matrices of the two elements, as shown schematically in Fig. 3. One can easily prove that the transmission and reflection matrices for the pair of elements, denoted by $\mathbf{Q}(n, n+1)$, are

$$\begin{aligned}
\mathbf{Q}^{\mathrm{I}}(n,n+1) &= \mathbf{Q}^{\mathrm{I}}(n+1)\left[\mathbf{I}-\mathbf{Q}^{\mathrm{II}}(n)\mathbf{Q}^{\mathrm{III}}(n+1)\right]^{-1}\mathbf{Q}^{\mathrm{I}}(n)\,,\\
\mathbf{Q}^{\mathrm{II}}(n,n+1) &= \mathbf{Q}^{\mathrm{II}}(n+1)+\mathbf{Q}^{\mathrm{I}}(n+1)\mathbf{Q}^{\mathrm{II}}(n)\left[\mathbf{I}-\mathbf{Q}^{\mathrm{III}}(n+1)\mathbf{Q}^{\mathrm{II}}(n)\right]^{-1}\mathbf{Q}^{\mathrm{IV}}(n+1)\,,\\
\mathbf{Q}^{\mathrm{III}}(n,n+1) &= \mathbf{Q}^{\mathrm{III}}(n)+\mathbf{Q}^{\mathrm{IV}}(n)\mathbf{Q}^{\mathrm{III}}(n+1)\left[\mathbf{I}-\mathbf{Q}^{\mathrm{II}}(n)\mathbf{Q}^{\mathrm{III}}(n+1)\right]^{-1}\mathbf{Q}^{\mathrm{I}}(n)\,,\\
\mathbf{Q}^{\mathrm{IV}}(n,n+1) &= \mathbf{Q}^{\mathrm{IV}}(n)\left[\mathbf{I}-\mathbf{Q}^{\mathrm{III}}(n+1)\mathbf{Q}^{\mathrm{II}}(n)\right]^{-1}\mathbf{Q}^{\mathrm{IV}}(n+1)\,.
\end{aligned}\tag{57}$$

All matrices refer of course to the same ω and $\boldsymbol{k}_{\parallel}$. We note in particular that the waves on the left (right) of the pair of elements are referred to an origin at $-\boldsymbol{d}_l(n)$ $(+\boldsymbol{d}_r(n+1))$ from the centre of the nth $((n+1)$th) element.

It is obvious that we can repeat the process to obtain the transmission and reflection matrices of three elements, by combining those of the pair of elements with those of the third element; and that we can in similar fashion repeat the process to obtain the scattering matrices of a slice consisting of any finite number of elements.

The subroutines relevant to this section are ZGE, ZSU and PAIR.

Subroutines ZGE, ZSU are standard routines which solve linear systems of equations of the form $\mathbf{A}\boldsymbol{X} = \boldsymbol{B}$, where $\mathbf{A}$ is a complex square matrix and $\boldsymbol{X}$, $\boldsymbol{B}$ are complex column matrices. ZGE performs Gaussian elimination of the matrix $\mathbf{A}$. ZSU takes as input the reduced matrix $\mathbf{A}$ from ZGE and vector $\boldsymbol{B}$, and implements a standard back-substitution algorithm to calculate the column matrix $\boldsymbol{X}$ which is stored in $\boldsymbol{B}$.

Given the Q-matrices of two elements (the input matrices of each element are characterized as left (L) and right (R) with respect to the z-axis, and are denoted in the program as QIL, QIIL, QIIIL, QIVL and QIR, QIIR, QIIIR, QIVR, respectively), subroutine PAIR returns the corresponding matrices given by Eq. (57) for the pair of them. The matrix inversions which are involved in Eq. (57) are performed by subroutines ZGE,

ZSU. PAIR stores the output matrices again in the arrays QIL, QIIL, QIIIL, QIVL. In this way we reduce the number of the different arrays needed in order to couple **Q**-matrices (see also Section 3.2).

2.5. Scattering by a slab

A slab may consist of a single slice and in this case the **Q**-matrices of the slab are those of the slice as defined in Section 2.4. However, a slab may consist of a number of identical slices stacked together along the z-axis (normal to the surface of the slab). We assume that the slab consists of 2^N slices, where $N = 0, 1, 2, \ldots$.

Having calculated the **Q**-matrix elements of a single slice, we obtain those of the slab by a doubling-layer scheme as follows: we first obtain the **Q**-matrix elements of two consecutive slices in the manner described in Section 2.4, then using as units the **Q**-matrix elements of a pair of slices, we obtain those of four consecutive slices, and in this way, by doubling the number of slices at each stage we finally obtain the **Q**-matrix elements of the 2^N slices of the slab. If the slab is embedded in a different homogeneous medium, the scattering at the left and right interfaces is taken into account by coupling the above obtained **Q**-matrices with those of the left and right interfaces, viewed as scattering elements, as discussed in Section 2.4.

In summary, for a plane wave $\sum_{i'} [E_{\mathrm{in}}]^{+}_{\mathbf{g}'i'} \exp(\mathrm{i}\boldsymbol{K}^{+}_{\mathbf{g}'_i} \cdot (\boldsymbol{r} - \boldsymbol{A}_L))\hat{\boldsymbol{u}}_{i'}$, incident on the slab from the left, we finally obtain a reflected wave $\sum_{\mathbf{g}i} [E_{\mathrm{rf}}]^{-}_{\mathbf{g}i} \exp(\mathrm{i}\boldsymbol{K}^{-}_{\mathbf{g}} \cdot (\boldsymbol{r} - \boldsymbol{A}_L))\hat{\boldsymbol{u}}_i$ on the left of the slab and a transmitted wave $\sum_{\mathbf{g}i} [E_{\mathrm{tr}}]^{+}_{\mathbf{g}i} \exp(\mathrm{i}\boldsymbol{K}^{+}_{\mathbf{g}} \cdot (\boldsymbol{r} - \boldsymbol{A}_R))\hat{\boldsymbol{u}}_i$ on the right of the slab, where $\boldsymbol{A}_L$ ($\boldsymbol{A}_R$) is the appropriate origin on the left (right) of the slab. We have

$$[E_{\mathrm{tr}}]^{+}_{\mathbf{g}i} = \sum_{i'} Q^{\mathrm{I}}_{\mathbf{g}i;\mathbf{g}'i'} [E_{\mathrm{in}}]^{+}_{\mathbf{g}'i'} , \tag{58}$$

$$[E_{\mathrm{rf}}]^{-}_{\mathbf{g}i} = \sum_{i'} Q^{\mathrm{III}}_{\mathbf{g}i;\mathbf{g}'i'} [E_{\mathrm{in}}]^{+}_{\mathbf{g}'i'} , \tag{59}$$

where the **Q**-matrix elements are those of the slab including the effects of the interfaces with an embedding medium, if such is the case.

When we have calculated the transmitted wave (58) and the reflected wave (59), corresponding to the given incident wave, we can obtain the transmittance $\mathcal{T}$ and the reflectivity $\mathcal{R}$ of the slab. $\mathcal{T}(\mathcal{R})$ is defined as the ratio of the flux of the transmitted (reflected) wave to the flux of the incident wave. Integrating the Poynting vector over the xy-plane, on the appropriate each time side of the slab, and taking the time average over a period $T = 2\pi/\omega$, we obtain

$$\mathcal{T} = \frac{\sum_{\mathbf{g}i} [E_{\mathrm{tr}}]^{+}_{\mathbf{g}i} \left([E_{\mathrm{tr}}]^{+}_{\mathbf{g}i}\right)^{*} K^{+}_{\mathbf{g}z}}{\sum_{i} [E_{\mathrm{in}}]^{+}_{\mathbf{g}'i} \left([E_{\mathrm{in}}]^{+}_{\mathbf{g}'i}\right)^{*} K^{+}_{\mathbf{g}'z}} ,$$

$$\mathcal{R} = \frac{\sum_{\mathbf{g}i} [E_{\mathrm{rf}}]^{-}_{\mathbf{g}i} \left([E_{\mathrm{rf}}]^{-}_{\mathbf{g}i}\right)^{*} K^{+}_{\mathbf{g}z}}{\sum_{i} [E_{\mathrm{in}}]^{+}_{\mathbf{g}'i} \left([E_{\mathrm{in}}]^{+}_{\mathbf{g}'i}\right)^{*} K^{+}_{\mathbf{g}'z}} , \tag{60}$$

where the $*$ sign denotes complex conjugation as usual. If the spheres of some planes absorb light, then the requirement of energy conservation implies that the absorbance $\mathcal{U}$ of the slab is

$$\mathcal{U} = 1 - \mathcal{T} - \mathcal{R} . \tag{61}$$

The subroutine relevant to this section is SCAT. It calculates the transmission, reflection and absorption coefficients, given by Eqs. (60) and (61), for a plane EM wave incident on the slab from the left. In calculating the sums of Eq. (60) waves with imaginary $K^{+}_{\mathbf{g}z}$ (decaying waves) are dropped, as they do not

transfer energy along the z-direction. We emphasize that the output of SCAT *must* satisfy Eq. (61). Therefore, if all the dielectric functions of the media making up the unit slice are real, the absorption coefficient must vanish; if it does not, it is most probably the case that the number of $\boldsymbol{g}$-vectors included in the calculation is not sufficient. Then the user must supply the input file with a larger value of RMAX in order to satisfy the above test.

2.6. *The complex band structure associated with a given surface of an infinite crystal*

We view the infinite crystal as a sequence of identical slices (parallel to the xy-plane) extending over all space (from $z = -\infty$ to $z = +\infty$). If (16) is the 2D space lattice for the slice, and $\boldsymbol{a}_3$ is a vector which takes us from a point in the Nth slice to an equivalent point in the $(N+1)$th slice, then $\{\boldsymbol{a}_1, \boldsymbol{a}_2, \boldsymbol{a}_3\}$ is a set of primitive vectors for the crystal.

We choose the reduced $\boldsymbol{k}$-zone of the corresponding reciprocal lattice as follows: $(\boldsymbol{k}_\parallel, k_z)$, where $\boldsymbol{k}_\parallel = (k_x, k_y)$ extends over the SBZ and $-|\boldsymbol{b}_3|/2 < k_z \leq |\boldsymbol{b}_3|/2$, where $\boldsymbol{b}_3 \equiv 2\pi \boldsymbol{a}_1 \times \boldsymbol{a}_2 / \boldsymbol{a}_1 \cdot (\boldsymbol{a}_2 \times \boldsymbol{a}_3)$. The complex band structure of the EM field, associated with the given surface of the above crystal, corresponds to mathematical solutions of Maxwell's equations which are generalized Bloch waves of given ω and given $\boldsymbol{k}_\parallel$ (see below).

In a region (of possibly infinitesimal thickness) between the Nth and the $(N+1)$th slices the wavefield, of given ω and $\boldsymbol{k}_\parallel$, has the form

$$\boldsymbol{E}(\boldsymbol{r}) = \sum_{\boldsymbol{g}} \left\{ \boldsymbol{E}_{\boldsymbol{g}}^{+}(N) \exp(\mathrm{i}\boldsymbol{K}_{\boldsymbol{g}}^{+} \cdot (\boldsymbol{r} - \boldsymbol{A}_N)) + \boldsymbol{E}_{\boldsymbol{g}}^{-}(N) \exp(\mathrm{i}\boldsymbol{K}_{\boldsymbol{g}}^{-} \cdot (\boldsymbol{r} - \boldsymbol{A}_N)) \right\} , \tag{62}$$

where $\boldsymbol{A}_N$ is the appropriate origin of coordinates; $\boldsymbol{K}_{\boldsymbol{g}}^{\pm}$ are defined by Eq. (21); and we remember that $q = \sqrt{\mu\epsilon}\,\omega/c$, where ϵ is the relative dielectric function and μ the relative magnetic permeability of the host medium in the given region.

The vector coefficients $\boldsymbol{E}_{\boldsymbol{g}}^{\pm}(N)$ are related to the $\boldsymbol{E}_{\boldsymbol{g}}^{\pm}(N+1)$ coefficients through the scattering properties of the Nth slice. We have

$$\begin{aligned} E_{\boldsymbol{g}i}^{-}(N) &= \sum_{\boldsymbol{g}'i'} Q^{\mathrm{IV}}_{\boldsymbol{g}i;\boldsymbol{g}'i'} E^{-}_{\boldsymbol{g}'i'}(N+1) + \sum_{\boldsymbol{g}'i'} Q^{\mathrm{III}}_{\boldsymbol{g}i;\boldsymbol{g}'i'} E^{+}_{\boldsymbol{g}'i'}(N) , \\ E_{\boldsymbol{g}i}^{+}(N+1) &= \sum_{\boldsymbol{g}'i'} Q^{\mathrm{I}}_{\boldsymbol{g}i;\boldsymbol{g}'i'} E^{+}_{\boldsymbol{g}'i'}(N) + \sum_{\boldsymbol{g}'i'} Q^{\mathrm{II}}_{\boldsymbol{g}i;\boldsymbol{g}'i'} E^{-}_{\boldsymbol{g}'i'}(N+1) , \end{aligned} \tag{63}$$

where $i = x, y, z$ and $\mathbf{Q}$ are the transmission/reflection matrix elements of the slice.

A generalized Bloch wave, by definition, has the property

$$\begin{aligned} &\boldsymbol{E}_{\boldsymbol{g}}^{\pm}(N+1) = \exp(\mathrm{i}\boldsymbol{k} \cdot \boldsymbol{a}_3)\, \boldsymbol{E}_{\boldsymbol{g}}^{\pm}(N) , \\ &\boldsymbol{k} = \left(\boldsymbol{k}_\parallel, k_z(\omega, \boldsymbol{k}_\parallel)\right) , \end{aligned} \tag{64}$$

where k_z is, for a given $\boldsymbol{k}_\parallel$, a function of ω, to be determined as follows.

Substituting Eq. (64) into Eq. (63) we obtain, after some algebra, the following system of equations:

$$\begin{pmatrix} \mathbf{Q}^{\mathrm{I}} & \mathbf{Q}^{\mathrm{II}} \\ -\left[\mathbf{Q}^{\mathrm{IV}}\right]^{-1}\mathbf{Q}^{\mathrm{III}}\mathbf{Q}^{\mathrm{I}} & \left[\mathbf{Q}^{\mathrm{IV}}\right]^{-1}\left[\mathbf{I} - \mathbf{Q}^{\mathrm{III}}\mathbf{Q}^{\mathrm{II}}\right] \end{pmatrix} \begin{pmatrix} \boldsymbol{E}^{+}(N) \\ \boldsymbol{E}^{-}(N+1) \end{pmatrix} = \exp(\mathrm{i}\boldsymbol{k} \cdot \boldsymbol{a}_3) \begin{pmatrix} \boldsymbol{E}^{+}(N) \\ \boldsymbol{E}^{-}(N+1) \end{pmatrix} , \tag{65}$$

where $\boldsymbol{E}^{\pm}$ are column matrices with elements $E^{\pm}_{\boldsymbol{g}_1 x}$, $E^{\pm}_{\boldsymbol{g}_1 y}$, $E^{\pm}_{\boldsymbol{g}_1 z}$, $E^{\pm}_{\boldsymbol{g}_2 x}$, $E^{\pm}_{\boldsymbol{g}_2 y}$, $E^{\pm}_{\boldsymbol{g}_2 z}$, ... In practice we keep $g_{\max}$ (denoted by IGMAX in the program) $\boldsymbol{g}$-vectors (those of the smallest magnitude) in which case $\boldsymbol{E}^{\pm}$ are

column matrices with $3g_{max}$ elements. The enumeration of the $\boldsymbol{g}$-vectors implied in the above definition of $\boldsymbol{E}^{\pm}$ is of course the same with the one we have introduced earlier in relation to the $\mathbf{Q}$-matrices (Section 2.2), each of which has $3g_{max} \times 3g_{max}$ elements; $\mathbf{I}$ is the $3g_{max} \times 3g_{max}$ unit matrix. For given $\boldsymbol{k}_{\|}$ and ω, we obtain $6g_{max}$ eigenvalues of k_z from the eigenvalues of the $6g_{max} \times 6g_{max}$ matrix on the left-hand side of Eq. (65). For given $\boldsymbol{k}_{\|}$ and ω, *one third of the corresponding eigensolutions are dropped* because the divergence of the electric field associated with them is not zero, as it must be in a free of charge space. The $4g_{max}$ eigenvalues $k_z(\omega; \boldsymbol{k}_{\|})$, corresponding to eigensolutions of Eq. (65) with zero divergence, looked upon as functions of real ω define, for each $\boldsymbol{k}_{\|}$, $4g_{max}$ lines in the complex k_z-space. Taken together they constitute the complex band structure associated with the given surface of the given crystal. A line of given $\boldsymbol{k}_{\|}$ may be real (in the sense that k_z is real) over certain frequency regions, and be complex (in the sense that k_z is complex) for ω outside these regions. Examples of such lines can be found in [9]. It turns out that for given $\boldsymbol{k}_{\|}$ and ω, out of the $4g_{max}$ eigenvalues of $k_z(\omega; \boldsymbol{k}_{\|})$ none or, at best, a few are real; the eigensolutions of Eq. (65) corresponding to them, represent propagating modes of the EM field in the given crystal. The remaining eigenvalues of $k_z(\omega; \boldsymbol{k}_{\|})$ are complex and the corresponding eigensolutions represent evanescent waves. These have an amplitude which increases exponentially in the positive or negative z-direction and, unlike the propagating waves, do not exist as physical entities in the infinite crystal. However, they are an essential part of physical solutions of the EM field in a semi-infinite crystal (extending from $z = -\infty$ to $z = 0$) or in a slab of finite thickness.

A region of frequency where propagating waves do not exist for given $\boldsymbol{k}_{\|}$ constitutes a frequency gap of the EM field for the given $\boldsymbol{k}_{\|}$. If over a frequency region no propagating wave exists whatever the value of $\boldsymbol{k}_{\|}$, then this region constitutes an (absolute) frequency gap, also called a photonic gap.

It is worth noting that because the eigenvalues of Eq. (65) are of the form $\exp(i\boldsymbol{k} \cdot \boldsymbol{a}_3)$, values of k_z differing by an integral multiple of $|\boldsymbol{b}_3|$ correspond to the same eigensolution, in accordance with the periodicity of the band structure in $\boldsymbol{k}$-space.

It is also worth noting that, when there is a plane of mirror symmetry associated with the surface under consideration, the eigensolutions (Bloch waves) of Eq. (65) appear in pairs: $k_z(\omega; \boldsymbol{k}_{\|})$ and $-k_z(\omega; \boldsymbol{k}_{\|})$.

Finally, we should point out that $k_z(\omega; \boldsymbol{k}_{\|})$ (for given $\boldsymbol{k}_{\|}$) is purposefully presented as a plot of $\omega a/c$ versus $2k_z/|\boldsymbol{b}_3|$, where a is the lattice constant of the crystal and c the velocity of light in vacuum, because in this way the results are applicable to different ranges of frequency of the EM field, provided that the size of the unit cell of the crystal is scaled accordingly.

The main subroutines relevant to this section are CNAA and BAND.

Subroutine CNAA along with CBABK2, CBAL, COMHES, COMLR2, ERRCHK, ONECHK, ERRPRT, ERXSET, ERRGET, ERSTGT are standard subroutines of the EISPACK library and compute the eigenvalues and the corresponding eigenvectors of an arbitrary complex square matrix. Users may use the algebraic-manipulation subroutines they prefer.

Subroutine BAND solves the eigenvalue problem defined by Eq. (65). The square matrix on the left-hand side of Eq. (65) is constructed using the subroutines ZGE, ZSU and diagonalised by CNAA. From the eigenvalues we obtain the values of k_z in dimensionless form: $\tilde{k}_z = 2k_z/|\mathbf{b}_3|$. Therefore, the real part of $\tilde{k}_z$ varies from -1 to 1. The $6g_{max}$ values of $\tilde{k}_z$ are stored in the array AKZ. The calculated eigenvectors are stored in the array COMVEC. Two filters are passed to COMVEC and AKZ: (a) it is determined whether or not an eigenvector of the electric field satisfies the zero-divergence condition, (b) the propagating solutions ($\tilde{k}_z$ real) are selected. The question which arises in practice is: how close to zero the calculated divergence of the electric field and the calculated imaginary part of $\tilde{k}_z$ must be to be considered as zero for practical purposes? After many test runs for various structures, we have concluded that in both cases a numerical value smaller than 10^{-2} should be taken as zero. However, this number is not to be taken always as a constant: it must be such that $2g_{max}$ of the solutions are discarded. This means that there is a dependence upon g_{max} but in most cases our choice of 10^{-2} is valid. If there are no propagating solutions ($\tilde{k}_z$ real) for a given frequency, the program prints out $\tilde{k}_z$ (a complex quantity) for the evanescent wave with the smallest $|\mathrm{Im}(\tilde{k}_z)|$ for the given ω and $\boldsymbol{k}_{\|}$.

3. Program description

MULTEM is a FORTRAN computer code which calculates the complex band structure associated with a given surface (crystallographic plane) of an infinite photonic crystal, and the transmission, reflection and absorption coefficients of a slab of the crystal. The structures that the program can deal with have been described in Section 1. The program consists of 29 subroutines and 4 functions.

3.1. Description of input data

Input data are read from unit 10. Output data are directed to the standard output unit 6, as well as to the output files in units 8 (transmission, reflection and absorption results) and 9 (band-structure results) for further use. In the following we explain the meaning of the input variables, in the order they are read from the input file (unit 10).

The integer variable KTYPE specifies the type of calculation the user wishes to perform. For KTYPE = 1,2 the program calculates the transmission, reflection and absorption coefficients of a finite slab. For KTYPE = 1 one specifies the direction of the incident EM wave by the polar angles of incidence θ and ϕ; while for KTYPE = 2 the incident wave is specified by $\boldsymbol{q}_{\parallel}$ and the frequency. For KTYPE = 3 the program calculates the complex band structure of the infinite crystal for a given $\boldsymbol{k}_{\parallel}$. The integer variable KSCAN decides whether to scan over frequencies (= 1) or wavelengths (= 2). KEMB (integer variable) indicates the presence (= 1) or absence (= 0) of an embedding medium and it is not effective if KTYPE = 3. LMAX is the cutoff value of the angular momentum in the spherical-wave expansions and takes integer values from 1 to 7.

NCOMP (integer variable) is the number of components in the unit slice and NUNIT (integer variable) specifies the number of unit slices (=2**(NUNIT−1)) in the slab. NUNIT is not effective if KTYPE = 3. ALPHA and ALPHAP (real variables) are the lengths, a and a', of the primitive vectors of the 2D lattice. a is taken along the x-axis and serves as the unit length. It must be set equal to 1. a' is given in units of a. FAB (real variable) is the angle (in deg) between the primitive vectors of the 2D lattice. The real variable RMAX defines the cutoff length, in units of $1/a$, for the 2D reciprocal-lattice vectors to be used in the plane-wave expansions. ZINF, ZSUP (real variables) are the minimum and maximum values of the frequency region or the wavelength region (according to the value of KSCAN), that is to be scanned. The frequency (ω) and the wavelength in vacuum (λ) of the incident radiation are given in program units: $\omega a/c$ and λ/a, respectively. NP (integer variable) is the number of (equally spaced) points between ZINF and ZSUP. AK(1), AK(2) (real variables) are the x, y-components of the wavevector of the incident wave, in units of $2\pi/a$. THETA, FI (real variables) are the polar angles of incidence in deg. POLAR is a character variable which specifies the polarization: S (the electric field parallel to the surface of the slab) or P (the electric field has a component normal to the surface of the slab); it is not effective for KTYPE = 3. FEIN (real variable) is the angle (in deg) specifying the direction of the polarization vector and it is effective only if KTYPE = 1,2 and in the case of normal incidence. Then follows the information for the NCOMP different components of the unit slice. For IT = 1 the component is a homogeneous plate and for IT = 2 a multilayer of spherical particles.

In the case of a homogeneous plate the program reads the following input data: D (real variable) which is the width of the homogeneous plate in units of a; MU1, EPS1, MU2, EPS2, MU3, EPS3 (complex variables) which are the values of the relative magnetic permeability and dielectric function of the plate (2) and the two semi-infinite media on its left (1) and its right (3), at the given frequency[3]; DL, DR (real variables) which are the three-dimensional position vectors defining the origins with respect to which the waves on the left and on the right of the plate are referred to. DL,DR are directed from left to right (see Fig. 2) and are given in

[3] In the distributed version of the program $\epsilon(\omega)$ and $\mu(\omega)$ are constants independent of ω. However, making ϵ and μ functions of ω constitutes a trivial extension.

units of a. We note that the case D=0 corresponds to an interface between two different homogeneous media and the choice of the relative magnetic permeability and dielectric function of the plate is in this case irrelevant.

In the case of a multilayer of spherical particles the program reads the following input data: MU1, EPS1 (complex variables) which are the values of the relative magnetic permeability and dielectric function at the given frequency (see footnote 3) of the homogeneous medium in which the spheres are embedded; NPLAN (integer variable) which is the number of non-primitive planes in the unit layer; and NLAYER (integer variable) which specifies the number of unit layers (=2**(NLAYER−1)) of the multilayer. For each non-primitive plane we give S (radius of spheres in units of a), MUSPH, EPSSPH (complex values of the relative magnetic permeability and dielectric function of the spheres at the given frequency, see footnote 3) and DL, DR (three-dimensional position vectors described previously).

After the input of the data for all the components of the unit slice, the program reads the information for the embedding medium, if present, in the case of a finite slab or the primitive translation vector of the unit slice in the case of a band-structure calculation. In particular, if KTYPE=1,2 and KEMB=1 the program reads MUEMB, EPSEMB (complex values of the relative magnetic permeability and dielectric function of the embedding medium at the given frequency, see footnote 3). Otherwise (KTYPE=3), it reads the three-dimensional position vector, $\boldsymbol{a}_3$ (AL), in units of a, which defines the primitive translation of the unit slice. We note that, although the dielectric functions and magnetic permeabilities of the various media are declared as complex variables in the program, only those referring to spheres and homogeneous plates are allowed to have a nonzero imaginary part.

3.2. *Main body of the program*

The main program first reads the input data as described in Section 3.1. We note that if the media of successive components (belonging to the same or successive slices) are not the same, an error message is activated and the program run is interrupted. After all input data are read, subroutine ELMGEN is called. Then, the primitive vectors of the direct and reciprocal lattice (AR1, AR2 and B1, B2, respectively) are constructed from ALPHA, ALPHAP, and FAB. By default, AR1 is taken to be parallel to the x-axis and equal to ALPHA. Next, subroutine LAT2D is called and the reciprocal-lattice vectors G are constructed. As the above calculations involve variables and arrays which are independent of frequency, the loop over frequencies/wavelengths begins after the calculation of the reciprocal-lattice vectors G. If KTYPE=1, AK is not given in the input file, as it is the case for KTYPE=2,3, but it is calculated from THETA, FI and the magnitude of the wavevector in vacuum (KAPPA0) for every frequency value.

If KTYPE=1 or 2, the program proceeds with the calculation of the polarization vector (EIN) of the incident plane wave from AK and KAPIN (the magnitude of the wavevector of the incident wave), according to the polarization mode (POLAR) defined in the input file. We note that if the magnitude of AK is less than EMACH, normal incidence and s-polarization are assumed. In this case EIN is given by the vector (COS(FEIN), SIN(FEIN), 0) where FEIN is defined in Section 3.1. The program calls subroutine REDUCE for the given AK and we obtain IG0 and the reduced AK. From EIN, the column vector EINCID ($[E_{in}]^{+}_{g_t}$) to be used in subroutine SCAT is constructed. It has 3*IGMAX elements which are all zero except those at the positions IG0+1, IG0+2, IG0+3 which are equal to the coordinates of EIN. If KTYPE=3, EINCID is not needed and subroutine REDUCE is called to obtain the reduced wavevector $\boldsymbol{k}_{\|}$, returned in array AK.

Next, the construction of the transmission/reflection matrices of the unit slice takes place. In order to reduce the number of arrays used when performing the matching of successive **Q**-matrices, we employ the following procedure: when the unit slice consists of a number of different components, the program begins with the construction of the **Q**-matrices of the first (from the left) component, which are stored in the arrays QIL, QIIL, QIIIL, QIVL. We shall denote these arrays collectively by QL for convenience. If the component is a homogeneous slab, subroutine HOSLAB is called. If the component is a multilayer of spheres, PCSLAB is called for the first non-primitive plane of the unit layer and stores the corresponding matrices in QL. Unless

the unit layer consists of one plane, PCSLAB is called for the treatment of the second (non-primitive) plane and the results are stored in QR, which denotes collectively the arrays QIR, QIIR, QIIIR, QIVR. Then PAIR combines the matrices QL and QR to produce the **Q**-matrices of the pair of planes which are stored in QL. These are combined with the matrices QR of the third (non-primitive) plane to yield a new set of QL, and so on. This procedure is repeated for all planes of the unit layer. Should the first component consist of a number (2**(NLAYER−1)) of identical unit layers, we feed PAIR with QL for both input left and right **Q**-matrices and this is repeated for (NLAYER−1) times. This doubling-layer algorithm has the following structure:

do for i=1 to NLAYER−1
  call PAIR for QL=QL and QR=QL
enddo

In any case, the **Q**-matrices of the first component of the unit slice are finally stored in QL. Then, the program proceeds to the second component by following the same algorithm employed for the first one. But now, the resulting matrices are stored in QR. In addition to this, the program uses a set of working arrays (WL) in the place of QL so that no information concerning the first component, which is stored in QL, is lost. Once the **Q**-matrices for the first (QL) and the second (QR) component are calculated, subroutine PAIR performs the coupling between them and returns a new set of QL. These are coupled with the corresponding matrices (QR) of the third component and so on for all the components of the unit slice. When PAIR is called for the last time, the transmission/reflection matrices of the unit slice are constructed.

After it has calculated the **Q**-matrices of the unit slice, the program proceeds to the calculation of the complex band structure of the infinite crystal or to the calculation of the transmission, reflection and absorption coefficients of a finite slab, according to the value of KTYPE In the first case, subroutine BAND is called. Otherwise, the doubling-layer algorithm described above is employed to construct the **Q**-matrices of a slab consisting of 2**(NUNIT−1) unit slices. If KEMB = 1, the **Q**-matrices of the slab are coupled first with those of the right-end interface and then with those of the left-end interface to obtain the **Q**-matrices of the slab in the embedding medium. We remember that, by construction, the left medium of the right-end interface is the same with the right medium of the left-end interface (for an example, see Section 4). Finally, subroutine SCAT returns the transmission, reflection and absorption coefficients. A flowchart of the main program is schematically shown in Fig. 4.

3.3. Subroutine PCSLAB

Subroutine PCSLAB computes the transmission/reflection matrices for a plane of spheres embedded in a homogeneous host medium, according to Eqs. (46). The results are stored in the arrays QI, QII, QIII and QIV. PCSLAB calls the following subroutines and functions: XMAT, ELMGEN, BLM, CERF, SPHRM4, TMTRX, BESSEL, CNWF01, DLMHKG, PLW, CODD, CEVEN, SETUP. Here we provide a brief description of the principal subroutines and functions and explain their role within PCSLAB.

Subroutine XMAT, along with ELMGEN, BLM, and CERF, computes the matrix element $Z_{\ell m;\ell' m'}$, given by Eqs. (27)–(30). The computer algorithm implements formulae given by Kambe [17] which transform, in the manner of Ewald, the sum over the 2D space lattice in Eq. (27) into two sums, the one over the space lattice and the second over its reciprocal lattice defined by Eq. (17). The calculation involves the complex error function [13], which is provided by the function CERF. The constant coefficients given by Eq. (29) are computed by the subroutine ELMGEN and stored in the array ELM. Since these coefficients do not depend on the lattice and frequency, ELMGEN is called once, in the beginning of the main program. More details and the subroutines themselves can be found in [15]. We note that XMAT takes advantage of the property (31) and by reordering the matrix elements of **Z** transforms it to a block-diagonal form. In this way, **Z** is reduced to two submatrices which correspond to $\ell + m$ and $\ell' + m'$ both even and to $\ell + m$ and $\ell' + m'$ both odd. These are stored in the arrays XEVEN and XODD, of dimensions $(\ell_{\max} + 2)(\ell_{\max} + 1)/2 \times (\ell_{\max} + 2)(\ell_{\max} + 1)/2$

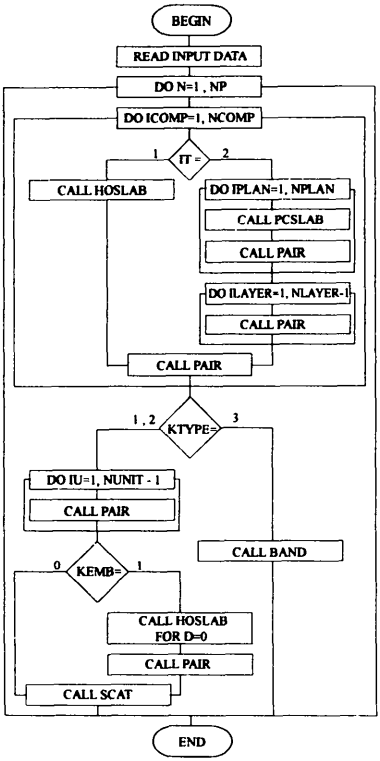

Fig. 4. A flowchart showing the structure of the main body of the program.

and $(\ell_{max}+1)\ell_{max}/2 \times (\ell_{max}+1)\ell_{max}/2$, respectively. By defining

$$e_0 = (\ell^2 + 2\ell + m + 2)/2 \quad \text{and} \quad o = (\ell^2 + m + 1)/2, \tag{66}$$

one can tabulate the matrix elements contained in XEVEN and XODD using the indices e_0, e_0' and o, o', respectively. We note that the (running) index e_0 counts also matrix elements with subscripts $(\ell, m) = (0, 0)$ because the array XEVEN contains such elements. When these elements are omitted, the index $e = e_0 - 1$ is used instead of e_0. The functions CEVEN and CODD, for given ℓ, m, ℓ', m', calculate the indices e_0, e_0' or o, o' according to Eq. (66) and return the corresponding matrix element of XEVEN or XODD, respectively.

The principal task performed by PCSLAB is the solution of the linear system of Eqs. (36). One can easily show, using the properties (32) of $\mathbf{\Omega}$ and rearranging Eqs. (36), that this system can be reduced to two systems of $\ell_{max}(\ell_{max}+2)$ equations as follows:

$$\begin{pmatrix} \mathbf{I} - \left[\mathbf{T}^E \boldsymbol{\Omega}^{EE}\right]_{oo'} & \left[\mathbf{T}^E \boldsymbol{\Omega}^{EH}\right]_{oe'} \\ \left[\mathbf{T}^H \boldsymbol{\Omega}^{HE}\right]_{eo'} & \mathbf{I} - \left[\mathbf{T}^H \boldsymbol{\Omega}^{HH}\right]_{ee'} \end{pmatrix} \begin{pmatrix} b^{+E}_{o'} \\ b^{+H}_{e'} \end{pmatrix} = \begin{pmatrix} \left[\mathbf{T}^E \boldsymbol{a}^{0E}\right]_o \\ \left[\mathbf{T}^H \boldsymbol{a}^{0H}\right]_e \end{pmatrix},$$

$$\begin{pmatrix} \mathbf{I} - \left[\mathbf{T}^H \boldsymbol{\Omega}^{HH}\right]_{oo'} & \left[\mathbf{T}^H \boldsymbol{\Omega}^{HE}\right]_{oe'} \\ \left[\mathbf{T}^E \boldsymbol{\Omega}^{EH}\right]_{eo'} & \mathbf{I} - \left[\mathbf{T}^E \boldsymbol{\Omega}^{EE}\right]_{ee'} \end{pmatrix} \begin{pmatrix} b^{+H}_{o'} \\ b^{+E}_{e'} \end{pmatrix} = \begin{pmatrix} \left[\mathbf{T}^H \boldsymbol{a}^{0H}\right]_o \\ \left[\mathbf{T}^E \boldsymbol{a}^{0E}\right]_e \end{pmatrix}, \tag{67}$$

where, for example, the matrix elements $\left[\mathbf{T}^E \boldsymbol{\Omega}^{EH}\right]_{oe'}$ correspond to the matrix elements $T^E_l \Omega^{EH}_{lm;l'm'}$ with $\ell + m$ odd and $\ell' + m'$ even (ordered according to the indices o and $e' = e'_0 - 1$).

Subroutine SETUP constructs the square matrices on the left-hand sides of Eqs. (67) and stores them in the arrays XXMAT1 and XXMAT2. For this purpose it uses the arrays TE and TH, computed by TMTRX, BESSEL and CNWF01 as described in Section 2.1; and the arrays XEVEN and XODD, computed by XMAT, from which the $\boldsymbol{\Omega}$-matrices are calculated by straightforward implementation of Eqs. (26).

The vectors on the right-hand sides of Eqs. (67) are constructed in a straightforward manner from TE, TH and AE, AH. The latter arrays contain the quantities $A^{0E}_{lm;l'}(\boldsymbol{K}^{s'}_{\boldsymbol{g}'})$, $A^{0H}_{lm;l'}(\boldsymbol{K}^{s'}_{\boldsymbol{g}'})$, as given by Eqs. (11). They are computed by subroutines PLW and SPHRM4, as described in Section 2.1. The arrays BMEL1 and BMEL2 contain the right-hand sides of Eqs. (67). Subroutine PCSLAB proceeds further by solving the linear systems (67) for $s' = +$ and all $\boldsymbol{g}'$ and i' using the subroutines ZGE and ZSU which have been described in Section 2.4. The resulting solutions $b^{+P}_{im}(+, \boldsymbol{g}', i')$ (returned in the arrays BMEL1, BMEL2), together with $\boldsymbol{\Delta}^P_{lm}(\boldsymbol{K}^+_{\boldsymbol{g}})$ (computed by subroutine DLMKG according to Eq. (44)), are used to calculate the matrix elements $M^{s+}_{\boldsymbol{g}i;\boldsymbol{g}'i'}$ according to Eq. (43). The matrix elements $M^{s-}_{\boldsymbol{g}i;\boldsymbol{g}'i'}$ are deduced from $M^{s+}_{\boldsymbol{g}i;\boldsymbol{g}'i'}$ using the symmetry relations (45). Finally, by multiplying $M^{ss'}_{\boldsymbol{g}i;\boldsymbol{g}'i'}$ with the appropriate phase factors which contain the position vectors $\boldsymbol{d}_l$, $\boldsymbol{d}_r$ (DL, DR) according to Eq. (46), all the **Q**-matrix elements are calculated.

4. Test run

For the test run we chose an heterostructure which has the unit slice shown in Fig. 5. This consists of four components (NCOMP = 4) which have a common 2D periodicity in the xy-plane: a square lattice (ALPHA = 1, ALPHAP = 1, FAB = 90). We note that all the materials have a magnetic permeability equal to unity.

The first component consists of two planes of identical spheres (IT = 2, NPLAN = 2, NLAYER = 1), of relative dielectric constant EPSSPH = 5.0 and radius S = 0.35a, embedded in a host medium of relative dielectric constant EPS1 = 2.0. The spheres in these two planes are arranged on two square lattices of the same lattice constant, a, but displaced relative to each other by the 2D vector $a(1/2, 1/2)$. The width of the component is 1.4a. The first (second) plane of spheres is situated at a distance 0.4a from the left(right)-end of the component, so that the distance between the two planes equals 0.6a. In accordance with the above structure of the first component, we put $\boldsymbol{d}_l = a(0, 0, 0.4)$ and $\boldsymbol{d}_r = a(0.25, 0.25, 0.3)$ for the first plane, and $\boldsymbol{d}_l = a(0.25, 0.25, 0.3)$, $\boldsymbol{d}_r = a(0.25, 0.25, 0.4)$, for the second plane of spheres.

It is convenient to introduce next the third component of the unit slice. This consists of one plane of spheres (IT = 2, NPLAN = 1, NLAYER = 1) of relative dielectric constant EPSSPH = 5.0 and radius S = 0.25a, embedded in a host medium of relative dielectric constant EPS1 = 7.0. The spheres are arranged on a square lattice, identical to that of the first plane of the first component. The width of the component is 0.6a and the plane of spheres is at the centre of the component. We put $\boldsymbol{d}_l = a(0.25, 0.25, 0.3)$ and $\boldsymbol{d}_r = a(0, 0, 0.3)$.

Since the host media of the first and third components are not the same, we must take into account the scattering at their interface. Thus we introduce a second component in the unit slice which is formally a

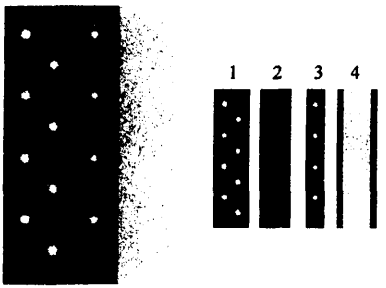

Fig. 5.

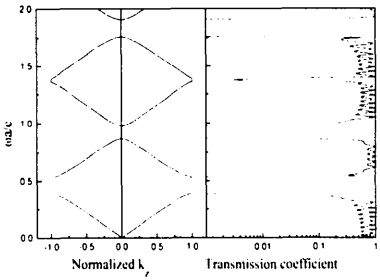

Fig. 6.

Fig. 5. The unit slice used in the test run. The unit slice consists of four different components as shown. The width of the darker regions of the fourth component is infinitesimally small.

Fig. 6. The complex photonic band structure of the infinite crystal corresponding to the unit slice of Fig. 5, for $k_{\parallel} = 0$ and the corresponding transmittance curve of a slab consisting of 32 unit slices. The dotted lines give the imaginary part of $\tilde{k}_z$, for the evanescent waves of the smallest $|\mathrm{Im}(\tilde{k}_z)|$.

homogeneous plate (IT = 1) with width D = 0. We take EPS1 = 2.0, EPS3 = 7.0 and EPS2 = 1.1; we remember that in the case of D = 0 (interface) the choice of EPS2 is immaterial. $\boldsymbol{d}_l$ and $\boldsymbol{d}_r$ are taken to be zero. The fourth component is again a homogeneous plate (IT = 1) with D = 1.0, EPS1 = 7.0, EPS2 = 9.0, EPS3 = 2.0, and $\boldsymbol{d}_l = \boldsymbol{d}_r = 0$. It can be verified that the present choice of the position vectors $\boldsymbol{d}_l$ and $\boldsymbol{d}_r$ for all the elements leads from a point at the left-end interface to an equivalent point at the right-end interface of the unit slice.

We calculated the transmission, reflection and absorption coefficients for a slab consisting of 32 unit slices (NUNIT = 6) as well as the complex band structure of the corresponding infinite crystal for AK(1) = AK(2) = 0. We scan over frequencies (KSCAN = 1) from ZINF = 0 to ZSUP = 2.0, with a step of 10^{-2} (NP = 201). For the transmission calculation (KTYPE = 2) we take POLAR = S; but had we taken POLAR = P, the results would be exactly the same in the present case of normal incidence. FEIN is taken to be zero. Furthermore, the slab is embedded (KEMB = 1) in air (EPSEMB = 1). For the band structure calculation (KTYPE = 3) the relevant primitive translation vector is AL = (0, 0, 3).

We use RMAX = 16, so that the 21 first reciprocal-lattice vectors are taken into account, while in the angular-momentum expansions we use a cutoff value LMAX = 4. The above values of LMAX and RMAX are sufficient for the given range of frequencies to obtain convergence. If the distance between successive planes was smaller and/or the frequencies higher, we would need a larger number (IGMAX) of reciprocal-lattice vectors. We note however that a larger value for RMAX must be accompanied by a larger value for LMAX; otherwise convergence is poor. In other words, if the electric field is described by a large number of terms in the spherical-wave expansions, a correspondingly large number of terms must be kept in the plane-wave expansions and vice versa, in order to retain an accurate description of the field.

The results stored in the output files in units 8 and 9 are shown in Fig. 6. We notice that the calculated absorption coefficient, obtained from Eq. (61), vanishes (it is of the order of 10^{-13}) and that the transmission minima are in perfect agreement with the frequency band gaps. Each transmission minimum is accompanied by satellite peaks which result from the finite size of the slab (Fabry-Perot-like oscillations).

For the sake of economy in the presentation only a fraction of the actual output data appears in the printouts of the output files. We note that in the printout of the band structure, giving the $\tilde{k}_z$-values for a given frequency ω, when $\tilde{k}_z$ is complex the imaginary part is printed below the real part.

References

[1] J. Joannopoulos, R. Meade, J. Winn, Photonic Crystals (Princeton, New York, 1995).
[2] E. Yablonovitch, J. Phys. 5 (1993) 2443.
[3] M. C. Wanke, O. Lehmann, K. Müller, Q. Wen, M. Stuke, Science 275 (1997) 1284.
[4] V. Karathanos, N. Stefanou, A. Modinos, J. Mod. Opt. 42 (1995) 619.
[5] C. Soukoulis, ed., Photonic Band Gap Materials (Kluwer, Dordrecht, 1996).
[6] J.B. Pendry, J. Mod. Opt. 41 (1994) 209;
J.B. Pendry, A. MacKinnon, Phys. Rev. Lett. 65 (1992) 2772;
P.M. Bell, J.B. Pendry, L. Martin-Moreno, A.J. Ward, Comput. Phys. Commun. 85 (1995) 306.
[7] A. Modinos, Physica A 141 (1987) 575.
[8] N. Stefanou, A. Modinos, J. Phys. 3 (1991) 8135.
[9] N. Stefanou, V. Karathanos, A. Modinos, J. Phys. 4 (1992) 7389.
[10] K. Ohtaka, Y. Tanabe, J. Phys. Soc. Jpn 65 (1996) 2265; 2276;
[11] Y. Qiu, K. M. Leung, L. Cavin, D. Kralj, J. Appl. Phys. 77 (1995) 3631.
[12] J. D. Jackson, Classical Electrodynamics (Wiley, New York, 1975).
[13] M. Abramowitz, I. Stegun, Handbook of Mathematical Functions (Dover, New York, 1965).
[14] Y.L. Luke, Algorithms for the Computation of Mathematical Functions (Academic Press, London, 1977).
[15] J.B. Pendry, Low Energy Electron Diffraction (Academic Press, London, 1974).
[16] A. Modinos, Field, Thermionic and Secondary Electron Emission Spectroscopy (Plenum Press, New York, 1984).
[17] K. Kambe, Z. Naturforsh. a 22 (1967) 322.

TEST RUN OUTPUT

```
            ***********************************************
            ********INPUT FILE FOR TRANSMISSION*********
            ***********************************************
  KTYPE = 2   KSCAN = 1   KEMB  = 1    LMAX = 4   NCOMP = 4   NUNIT = 6
 ALPHA =    1.000000  BETA =    1.000000   FAB =   90.000000  RMAX =   16.000000
  NP =  17  ZINF =   1.00000000  ZSUP =   2.000000000
  THETA/AK(1) =   0.00000000     FI/AK(2) =   0.00000000   POLAR =S     FEIN =   0.00

Give information for the "NCOMP" components

     IT  = 2
     MUMED =   1.00000000   0.00000000     EPSMED=   2.00000000   0.00000000
   NPLAN = 2  NLAYER = 1
       S =   0.35000000     MUSPH =   1.00000000   0.00000000     EPSSPH=   5.00000000   0.00000000
xyzDL 0.0  0.0  0.4
xyzDR 0.25 0.25 0.3
       S =   0.35000000     MUSPH =   1.00000000   0.00000000     EPSSPH=   5.00000000   0.00000000
xyzDL 0.25 0.25 0.3
xyzDR 0.25 0.25 0.4
     IT  = 1
  DSLAB        =   0.00000000
     MU1   =   1.00000000   0.00000000     EPS1  =   2.00000000   0.00000000
     MU2   =   1.00000000   0.00000000     EPS2  =   1.10000000   0.00000000
     MU3   =   1.00000000   0.00000000     EPS3  =   7.00000000   0.00000000
xyzDL 0.0  0.0  0.0
xyzDR 0 0  0.0  0.0
     IT  = 2
     MUMED =   1.00000000   0.00000000     EPSMED=   7.00000000   0.00000000
   NPLAN = 1  NLAYER = 1
       S =   0.25000000     MUSPH =   1.00000000   0.00000000     EPSSPH=   5.00000000   0.00000000
xyzDL 0.25 0.25 0.3
xyzDR 0.0  0.0  0.3
     IT  = 1
  DSLAB        =   1.00000000
     MU1   =   1.00000000   0.00000000     EPS1  =   7.00000000   0.00000000
     MU2   =   1.00000000   0.00000000     EPS2  =   9.00000000   0.00000000
     MU3   =   1.00000000   0.00000000     EPS3  =   2.00000000   0.00000000
xyzDL 0.0  0.0  0.0
xyzDR 0.0  0.0  0.0
     MUEMB =   1.00000000   0.00000000    EPSEMB =   1.00000000   0.00000000
```

```
            ********************************************
            *******INPUT FILE FOR BAND STRUCTURE********
            ********************************************
  KTYPE = 3   KSCAN = 1   KEMB  = 1    LMAX = 4   NCOMP = 4   NUNIT = 6
 ALPHA =    1.000000  BETA =    1.000000   FAB =   90.000000  RMAX =   16.000000
  NP = 17  ZINF =   1.00000000  ZSUP =   2.000000000
  THETA/AK(1) =   0.00000000     FI/AK(2) =   0.00000000   POLAR =S     FEIN =   0.00

Give information for the "NCOMP" components

     IT  = 2
     MUMED =   1.00000000   0.00000000     EPSMED=   2.00000000   0.00000000
   NPLAN = 2  NLAYER = 1
       S =   0.35000000     MUSPH =   1.00000000   0.00000000     EPSSPH=   5.00000000   0.00000000
xyzDL 0.0  0.0  0.4
xyzDR 0.25 0.25 0.3
       S =   0.35000000     MUSPH =   1.00000000   0.00000000     EPSSPH=   5.00000000   0.00000000
xyzDL 0.25 0.25 0.3
xyzDR 0.25 0.25 0.4
     IT  = 1
  DSLAB       =   0.00000000
     MU1   =   1.00000000   0.00000000     EPS1  =   2.00000000   0.00000000
     MU2   =   1.00000000   0.00000000     EPS2  =   1.10000000   0.00000000
     MU3   =   1.00000000   0.00000000     EPS3  =   7.00000000   0.00000000
xyzDL 0.0  0.0  0.0
xyzDR 0.0  0.0  0.0
     IT  = 2
     MUMED =   1.00000000   0.00000000     EPSMED=   7.00000000   0.00000000
   NPLAN = 1  NLAYER = 1
       S =   0.25000000     MUSPH =   1.00000000   0.00000000     EPSSPH=   5.00000000   0.00000000
xyzDL 0.25 0.25 0.3
xyzDR 0.0  0.0  0.3
     IT  = 1
  DSLAB       =   1.00000000
     MU1   =   1.00000000   0.00000000     EPS1  =   7.00000000   0.00000000
     MU2   =   1.00000000   0.00000000     EPS2  =   9.00000000   0.00000000
     MU3   =   1.00000000   0.00000000     EPS3  =   2.00000000   0.00000000
xyzDL 0.0  0.0  0.0
xyzDR 0.0  0.0  0.0
xyzAL 0.0  0.0  3.0
```

```
**************************************************
*** OUTPUT: TRANSMITTANCE/REFLECTANCE/ABSORBANCE ***
**************************************************
K_PARALLEL=     .000000     .000000     S POLARIZATION
COMPONENT NR. 1   TYPE:  PHOTONIC CRYSTAL
MU :   1.00000    .00000 |      1.00000    .00000      1.00000    .00000
EPS:   2.00000    .00000 |      5.00000    .00000      5.00000    .00000
  S:                              .35000                  .35000
                              1 UNIT LAYERS
COMPONENT NR. 2   TYPE:  HOMOGENEOUS PLATE
MU :   1.00000    .00000 |    1.00000    .00000 |    1.00000    .00000
EPS:   2.00000    .00000 |    1.10000    .00000 |    7.00000    .00000
COMPONENT NR. 3   TYPE:  PHOTONIC CRYSTAL
MU :   1.00000    .00000 |      1.00000    .00000
EPS:   7.00000    .00000 |      5.00000    .00000
  S:                              .25000
                              1 UNIT LAYERS
COMPONENT NR. 4   TYPE:  HOMOGENEOUS PLATE
MU :   1.00000    .00000 |    1.00000    .00000 |    1.00000    .00000
EPS:   7.00000    .00000 |    9.00000    .00000 |    2.00000    .00000
THE SAMPLE CONSISTS OF     32 UNIT SLICES

          PRIMITIVE LATTICE VECTORS
          AR1 = (      1.0000       .0000)
          AR2 = (       .0000      1.0000)
          UNIT VECTORS IN RECIPROCAL SPACE:
          B1  = (       .0000      6.2832)
          B2  = (     -6.2832       .0000)

 RECIPROCAL VECTORS     LENGTH
 1        0    0        .000000E+00
 2       -1    0        .628319E+01
 3        0   -1        .628319E+01
 4        1    0        .628319E+01
 5        0    1        .628319E+01
 6       -1    1        .888577E+01
 7        1   -1        .888577E+01
 8       -1   -1        .888577E+01
 9        1    1        .888577E+01
10        0    2        .125664E+02
11        0   -2        .125664E+02
12       -2    0        .125664E+02
13        2    0        .125664E+02
14        2   -1        .140496E+02
15       -2    1        .140496E+02
16       -1    2        .140496E+02
17        1   -2        .140496E+02
18       -2   -1        .140496E+02
19       -1   -2        .140496E+02
20        1    2        .140496E+02
21        2    1        .140496E+02

   FREQUENCY   TRANSMITTANCE  REFLECTANCE   ABSORBANCE
-------------------------------------------------------
  .100000E+01   .211294E+00   .788706E+00   .396350E-13
  .106250E+01   .940804E+00   .591957E-01   .938971E-13
```

112500E+01	.543944E+00	.456056E+00	.410[illegible]5-13
118750E+01	.722408E+00	.277592E+00	-.286438E-13
125000E+01	.718011E+00	.281989E+00	.129341E-12
131250E+01	.588369E+00	.411631E+00	-.695000E-13
137500E+01	.359722E-02	.996403E+00	-.949241E-13
143750E+01	.973861E+00	.261393E-01	.115515E-12
150000E+01	.544856E+00	.455144E+00	.320854E-13
156250E+01	.598532E+00	.401468E+00	.579536E-13
162500E+01	.974029E+00	.259715E-01	.124737E-12
168750E+01	.774661E+00	.225339E+00	-.990874E-14
175000E+01	.590934E+00	.409066E+00	.113687E-12
181250E+01	.183498E-13	.100000E+01	-.877076E-14
187500E+01	.781130E-12	.100000E+01	-.133227E-14
193750E+01	.880987E+00	.119013E+00	-.106859E-12
200000E+01	.815269E+00	.184732E+00	.779377E-13

```
   ******************************************************
   ************** OUTPUT: BAND STRUCTURE **************
   ******************************************************
  K_PARALLEL=      .000000      .000000
  COMPONENT NR. 1   TYPE:  PHOTONIC CRYSTAL
  MU :    1.00000     .00000 |        1.00000     .00000       1.00000     .00000
  EPS:    2.00000     .00000 |        5.00000     .00000       5.00000     .00000
    S:                                .35000                    .35000
                                   1 UNIT LAYERS
  COMPONENT NR. 2   TYPE:  HOMOGENEOUS PLATE
  MU :    1.00000     .00000 |     1.00000     .00000 |     1.00000     .00000
  EPS:    2.00000     .00000 |     1.10000     .00000 |     7.00000     .00000
  COMPONENT NR. 3   TYPE:  PHOTONIC CRYSTAL
  MU :    1.00000     .00000 |        1.00000     .00000
  EPS:    7.00000     .00000 |        5.00000     .00000
    S:                                .25000
                                   1 UNIT LAYERS
  COMPONENT NR. 4   TYPE:  HOMOGENEOUS PLATE
  MU :    1.00000     .00000 |     1.00000     .00000 |     1.00000     .00000
  EPS:    7.00000     .00000 |     9.00000     .00000 |     2.00000     .00000

            PRIMITIVE LATTICE VECTORS
            AR1 = (       1.0000        .0000)
            AR2 = (        .0000       1.0000)
            UNIT VECTORS IN RECIPROCAL SPACE:
            B1  = (        .0000       6.2832)
            B2  = (      -6.2832        .0000)

  RECIPROCAL VECTORS      LENGTH
 1        0    0        .000000E+00
 2       -1    0        .628319E+01
 3        0   -1        .628319E+01
 4        1    0        .628319E+01
 5        0    1        .628319E+01
 6       -1    1        .888577E+01
 7        1   -1        .888577E+01
 8       -1   -1        .888577E+01
 9        1    1        .888577E+01
10        0    2        .125664E+02
11        0   -2        .125664E+02
12       -2    0        .125664E+02
13        2    0        .125664E+02
14        2   -1        .140496E+02
15       -2    1        .140496E+02
16       -1    2        .140496E+02
17        1   -2        .140^96E+02
18       -2   -1        .140496E+02
19       -1   -2        .140496E+02
20        1    2        .140496E+02
21        2    1        .140496E+02


FREQUENCY        NORMALIZED K_Z
---------        --------------
.1000E+01     .1121E+00  .1121E+00 -.1121E+00 -.1121E+00
.1063E+01    -.2791E+00  .2791E+00  .2791E+00 -.2791E+00
.1125E+01    -.4263E+00  .4263E+00  .4263E+00 -.4263E+00
```

```
1188E+01    .5695E+00  .5695E+00 -.5695E+00 -.5695E+00
1250E+01    .7115E+00  .7115E+00 -.7115E+00 -.7115E+00
1313E+01    .8543E+00 -.8543E+00  .8543E+00 -.8543E+00
1375E+01   -.1000E+01 -.1000E+01
            .3456E-01 -.3456E-01
1438E+01   -.8735E+00 -.8735E+00  .8735E+00  .8735E+00
1500E+01   -.7292E+00 -.7292E+00  .7292E+00  .7292E+00
1563E+01   -.5853E+00 -.5853E+00  .5853E+00  .5853E+00
1625E+01   -.4388E+00 -.4388E+00  .4388E+00  .4388E+00
1688E+01   -.2849E+00  .2849E+00 -.2849E+00  .2849E+00
1750E+01    .9137E-01  .9137E-01 -.9137E-01 -.9137E-01
1813E+01   -.5078E-10 -.2143E-10
            .1608E+00 -.1608E+00
1875E+01    .2938E-06 -.7726E-11
            .1455E+00 -.1455E+00
1938E+01    .1511E+00  .1511E+00 -.1511E+00 -.1511E+00
2000E+01    .3269E+00  .3269E+00 -.3269E+00 -.3269E+00
```